AD-A063 867 BOLT BERANEK AND NEWMAN INC CAMBRIDGE MASS F/G 20/1
CALCULATION OF LOW FREQUENCY CAVITATION SOURCE STRENGTH OF MARI--ETC(U)
JUL 78 D S GREELEY

UNCLASSIFIED BBN-TM-459 NL

| OF |
AD
A063 867

END
DATE
FILMED
3--79
DDC

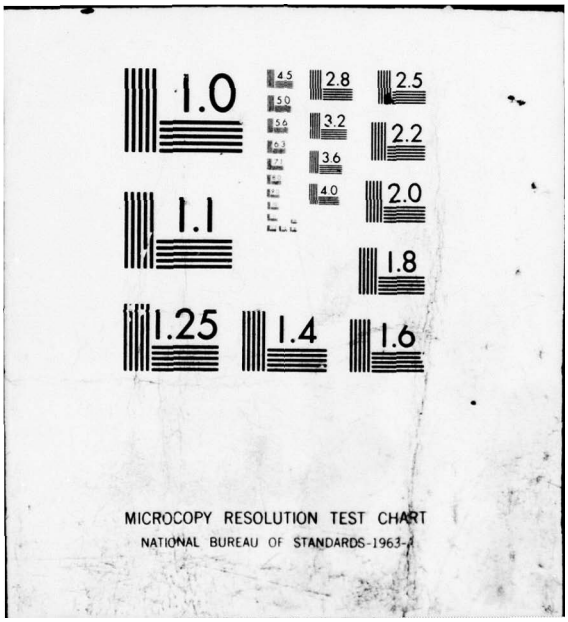
1.0
1.1
1.25
1.4
1.6
1.8
2.0
2.2
2.5
2.8
3.2
3.6
4.0
4.5
5.0
5.6
6.3
MICROCOPY RESOLUTION TEST CHART
NATIONAL BUREAU OF STANDARDS-1963-A

Bolt Beranek and Newman Inc.

LEVEL II

Technical Memorandum No. 459

Calculation of Low Frequency Cavitation Source Strength of Marine Propellers

D.S. Greeley

July 1978

Prepared for:
Naval Research Laboratory

(14) BBN-TM-459

TECHNICAL MEMORANDUM NO. 459

(6) CALCULATION OF LOW FREQUENCY CAVITATION SOURCE STRENGTH OF MARINE PROPELLERS.

(10) D. S. Greeley

(9) Technical memo.

(11) July ~~1978~~ 1978

(12) 66 p.

Submitted to:

Naval Research Laboratory
Washington, D.C.

Attention: Mr. Orest Diachok

Questions or comments regarding this memo should be addressed to Mr. Leslie M. Gray at:

Bolt Beranek and Newman Inc.
50 Moulton Street
Cambridge, Mass. 02138

060 400

lk

TABLE OF CONTENTS

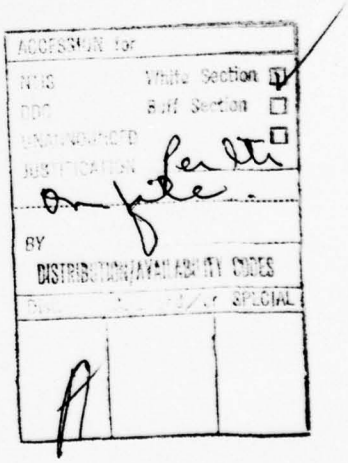

1.0 INTRODUCTION

1.1 Background

This memorandum documents recent improvements to ~~the~~ a model developed by Bolt Beranek and Newman (BBN) for the prediction of volume-time histories for sheet cavitation on the blades of merchant ship propellers, and the low frequency acoustic radiation resulting from these sheet cavitation volume fluctuations. This model is part of a larger effort directed at predicting the statistics of ocean ambient noise due to merchant shipping.

A description of the mechanics of sheet cavitation on propeller blades and the acoustic radiation resulting from fluctuations in sheet cavitation volume is given in an earlier report, BBN Tech Memo No. 319, ~~(Ref. 1)~~ and will not be repeated here. It is assumed that the reader is familiar with the contents of Tech Memo No. 319, which describes these processes and the approach used to model them.

1.2 Objectives and Scope

The previous version of our model considerably over-predicted the amount of cavitation present on propeller blades as they rotate through the uneven wakefield behind a single screw ship, and thus over-predicted the acoustic radiation resulting from these cavity fluctuations. As discussed in Reference 2, this over-prediction was attributed to three major factors:

- For determining the loading (lift) on the propeller blade, the previous model assumed that the blade could be replaced by a single "lifting line" of zero chord, and that the inflow at this lifting line was representative of the flow over the whole blade. Physical propellers have finite chord lengths and tend to "average" the inflow variations

over the chordwise extent of the blade, thus reducing the response of the blade to inflow variations.

- The previous model assumed that the propeller blade section could be replaced by a zero thickness flat plate when calculating the occurrence and extent of sheet cavitation. This will tend to over-predict the occurrence of cavitation, since real propellers are comprised of airfoil type sections with rounded leading edges and can tolerate moderate angle of attack fluctuations without provoking the occurrence of sheet cavitation.
- The previous model did not include the effect of cavitation on the lift of the propeller blade sections (cavitating lift-slope).

The present report documents four major items:

- Improvements to the model to overcome the shortcomings listed above.
- A sensitivity analysis to determine the influence of the input variables on the predicted cavitation noise.
- Comparison of measured cavitation line spectra from merchant ships with levels estimated using the current model.
- Discussion of shortcomings in the modeling process which require further investigation.

2.0 TECHNICAL APPROACH

The approach adopted for the calculation of the blade loading at each angular position in the wake is based on quasi-steady lifting-line theory, as described in Ref. 1. The details of the numerical lifting-line calculations have been changed somewhat from the description given in Ref. 1 due to numerical problems in the previous computer program. The new program has proven to be very reliable and shows rapid convergence to the solution of the inverse lifting line problem with no numerical instabilities evident.

2.1 Effects of Finite Blade Width

In order to account for the effect of finite blade width when calculating the loading on the blade, the inflow velocities are averaged over the chordwise extent of the blade in order to determine the axial wake velocity V_A, the tangential wake velocity V_T, and the geometric inflow angle β (see Fig. 2.1). Initially the averaging was done uniformly over the blade chord, i.e. the wake velocities near the leading and trailing edges of the blade were weighted equally in the averaging process. This did not seem to provide the correct response of the propeller blade to the wake-field. Since Brown (3) had shown the leading edge of the propeller blade to govern the generation of unsteady propeller forces, the averaging calculations were modified to weight the inflow velocities near the leading edge of the blade more heavily than those near the trailing edge. This appears to provide a better estimate of the propeller blade's response to the wake non-uniformities. Sasajima (4) has also applied this leading-edge weighting method to the quasi-steady estimation of unsteady propeller forces and found generally good agreement with experimental results and calculations done using very complete unsteady lifting surface theory (5). This wake averaging method with the averaging weighted toward the leading edge of the blade, has been adopted for the present work.

BASIC REQUIREMENT OF
LIFTING LINE THEORY:
C_L FROM ANGLE OF ATTACK MUST
EQUAL C_L FROM TRAILING VORTEX
SYSTEM.

$$C_L = \frac{\text{LIFT}}{\text{CHORD} \times \frac{\rho}{2} V^2}$$

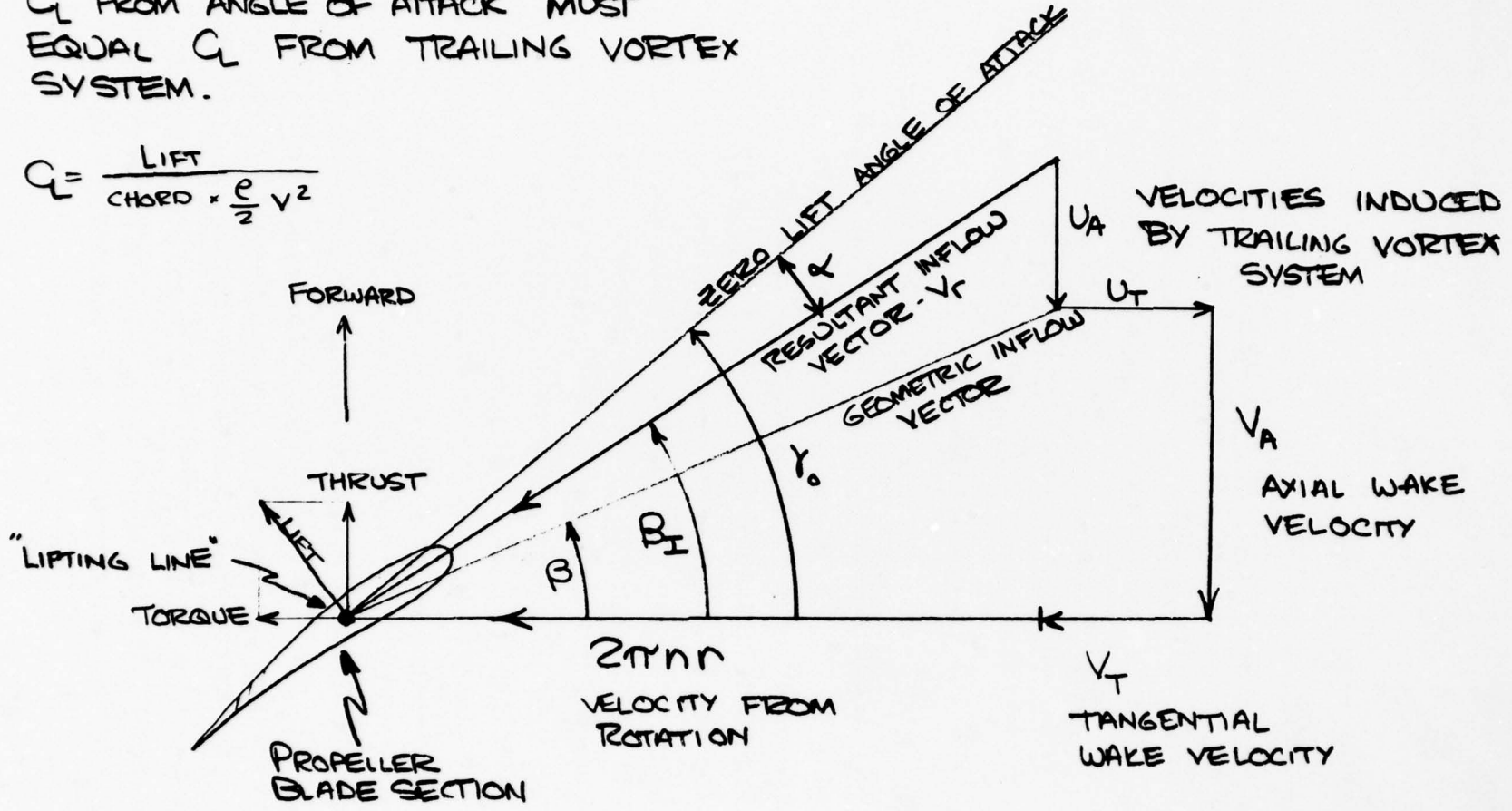

FIGURE 2.1

PROPELLER INFLOW REPRESENTATION

2.2 Propeller Blade Sections

Actual propeller blade sections are able to withstand a finite change in angle of attack ($\Delta\alpha$) without suffering leading edge sheet cavitation. The angle of attack, α that a given section can withstand is dependent on the cavitation number, σ

$$\sigma = \frac{P_o - P_V}{\frac{1}{2}\rho V^2} \tag{2.1}$$

P_o = ambient pressure

P_V = vapor pressure of fluid

ρ = fluid density

V = flow velocity

Graphically, this is represented by a cavitation "bucket" diagram, shown in Fig. 2.2. The "bucket" is the curve drawn on a α vs σ diagram showing the boundary between the region for which sheet cavitation will occur and the region of no cavitation. Note that the bucket width for a given section is dependent on the cavitation number σ.

The shape of the cavitation bucket for a propeller blade section is dependent on the thickness-to-chord (t/c) ratio, the type of thickness distribution, and the magnitude and shape of the camber distribution (curvature of the centerline of the blade section). For a given arbitrary blade section the bucket curve may be calculated, but the numerical calculations are quite lengthy, and outside the scope of the present work. The approach utilized here is to consult tabulated cavitation buckets for a given type of thickness and camber distribution and assume that these sections are representative of the type of blade sections found in the world's merchant ship propellers. The type of section used in the

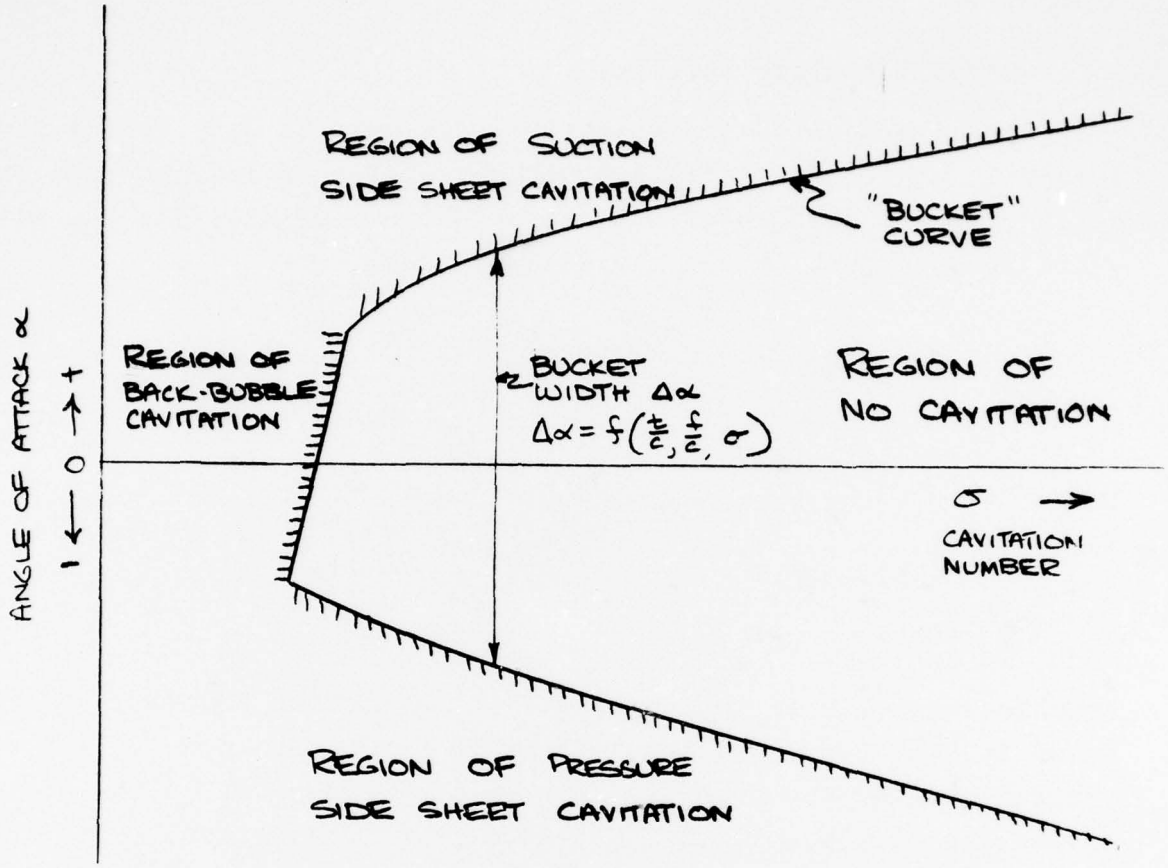

BUCKET CURVE FOR PROPELLER BLADE SECTION

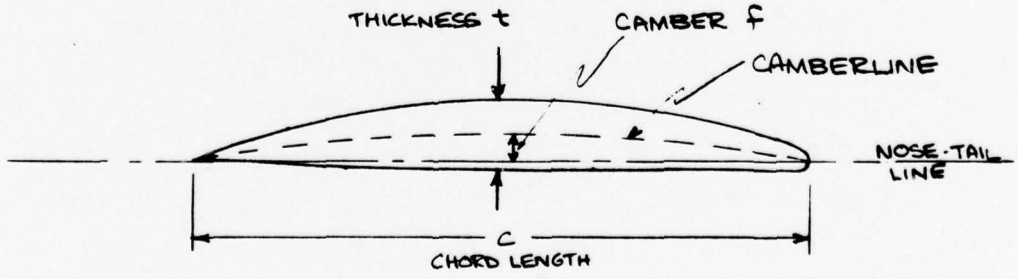

THICKNESS RATIO = t/c
CAMBER RATIO = f/c

TYPICAL PROPELLER BLADE SECTION

FIGURE 2.2

present work is the NACA 66 thickness distribution in conjunction with an a=0.8 type of camber distribution (Ref. 6). This type of section is widely used in marine propellers designed and built in the past few years. Very complete cavitation bucket diagrams are available for this section (Ref. 7), and the buckets were already available in numerical form (8) for use in our computer program, which saved considerable programming effort in the present work.

The NACA 66 section, whose properties have been incorporated into the present computer program, is more tolerant of angle of attack fluctuations than many types of blade sections used in the world's merchant ship propellers. However, since the thickness-to-chord (t/c) ratio is the major parameter which affects cavitation bucket width ($\Delta\alpha$) at a given cavitation number (σ), the cavitation buckets of other types of blade sections may be simulated by entering the NACA 66 bucket curves at a t/c ratio which is suitabily modified so that the resulting bucket width is that of the section under consideration. This modified t/c ratio is readily calculated.

In the computer program, the angle of attack α for each blade section of the propeller is determined by using quasi-steady lifting line theory to solve for the loading on the blade, as discussed in Sections 2.0 and 2.1. The cavitation number σ for each section is calculated from Equation 2.1. Then for each blade section along the blade, the NACA 66 bucket curves are entered with the proper values of α, σ, t/c, and camber ratio to determine whether or not sheet cavitation is present at that section.

2.3 Calculation of Cavity Extent and Cross Sectional Area

Once it has been determined that sheet cavitation is occurring at a particular blade section, the chordwise extent and cross-sectional area of the cavity at that radius are calculated using lin-

earized free-streamline cavitating foil theory (9-13). This theory assumes that the pressure field around the blade section which influences the cavitation extent and area is composed of two components: the pressure distribution associated with a flat plate at angle of incidence α, and the pressure distribution associated with a foil having a parabolic arc camberline of camber ratio λ, as shown in Figure 2.3. The *effective* camber of a blade section in non-uniform flow can be considered as being made up of two parts:

- The *geometric* camber of the actual blade section.
- The *induced* camber caused by the curvature of the flow over the blade chord.

Van Oossanen has shown (14) that induced camber is quite important in determining the cavitation characteristics of a propeller. We have adopted van Oossanen's method of calculating induced camber due to non-uniform inflow (15), and use the sum of the blade geometric camber and the induced camber in entering the cavitating foil calculations. The inclusion of this induced camber effect significantly improved the correlation between cavitation patterns predicted using our computer program and the cavitation patterns observed on model propellers in cavitation tunnels.

2.4 Effect of Cavitation on Lift (Cavitating Lift Slope)

Cavitation is known to alter the lift and drag characteristics of foil sections relative to the non-cavitating condition. Since the relationship between angle of attack and lift coefficient is used to solve for the loading on the blade, the effects of cavitation on lift slope should (in principle) be included in the quasi-steady solution for the blade loading. We originally anticipated that the inclusion of this effect would significantly alter the predicted cavitation volume history on the propeller. A re-examin-

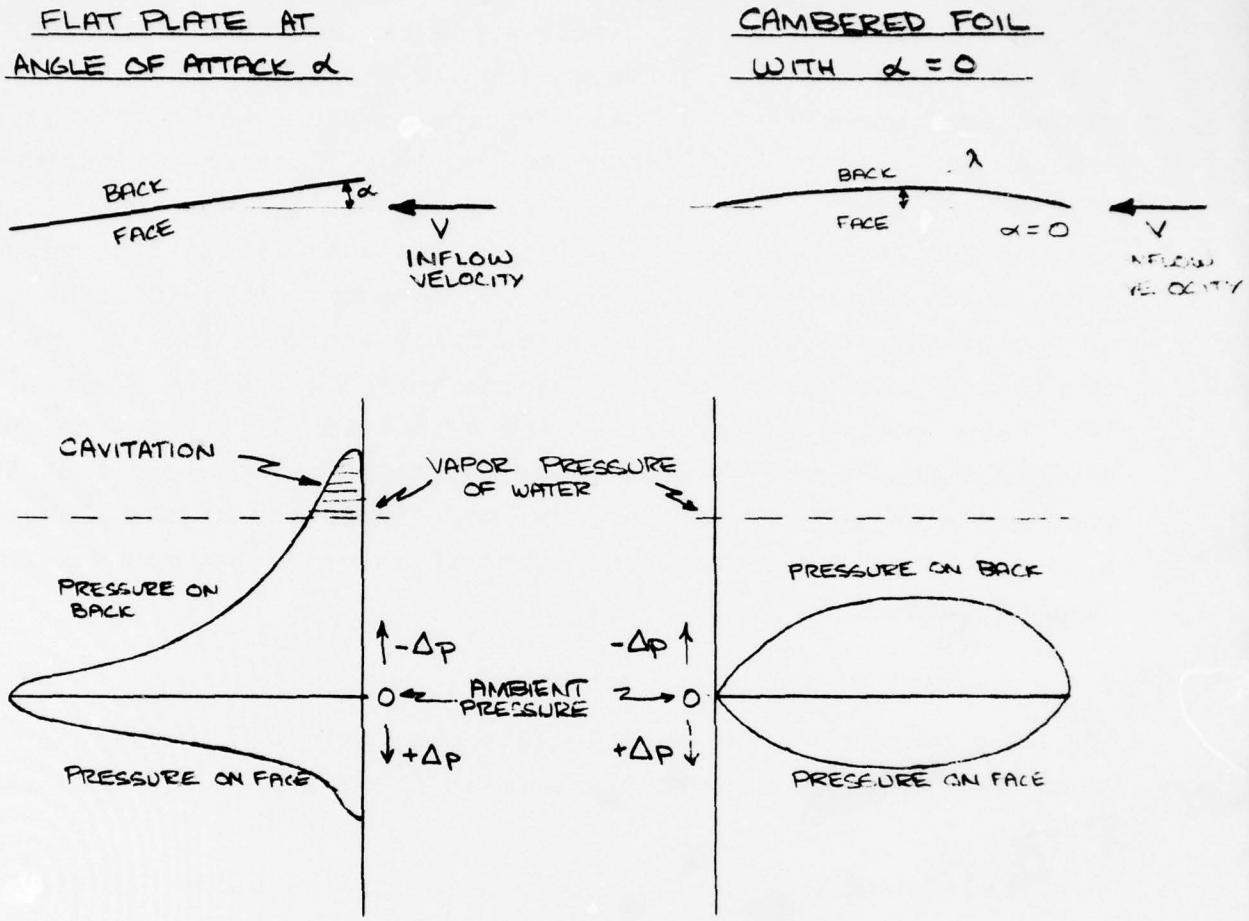

COMPARISON OF PRESSURE DISTRIBUTIONS AROUND FLAT PLATE & CAMBERED AIRFOILS, WHEN GENERATING EQUAL LIFT

FIGURE 2.3

ation of this problem during the present work now indicates that the effect of the cavitating lift slope on the final predicted volume history would be quite small, and the error involved with neglecting this effect is insignificant compared to other shortcomings inherent in the present method of estimating cavitation volume histories. Moreover, the inclusion of the cavitating lift slope leads to numerical instabilities in the lifting-line equations which may be very difficult to overcome. This author knows of no investigators who have successfully included the effects of cavitation in solving for the loading on the propeller blades. For these reasons the effect of the cavitating lift slope has not been included in the present work, and it is recommended that this phenomenon be ignored until other, more important effects have been accounted for in the estimation of sheet cavitation volume-time histories.

2.5 Summary of Analysis Procedure

The procedure used to calculate the cavitation volume on a propeller blade at a given position in the wakefield is summarized below.

A. For each of 9 blade sections along the blade, examine the wake velocities over the chordwise extent of the blade and determine the weighted average inflow angle β, axial velocity V_A, and tangential velocity V_T. The induced camber due to the curvature of the flow is also calculated at this time.

B. Using the inflow quantities calculated in Step A and the known blade geometry, calculate the blade loading and corresponding blade section angles of attack using quasi-steady lifting line theory.

C. For each blade section, consult the appropriate cavitation bucket curve to determine whether or not sheet cavitation is occurring at that section.

D. For each blade section at which sheet cavitation is predicted to occurr, calculate the chordwise extent and the cross sectional area of the sheet cavity using free-streamline cavitating foil theory.

E. Integrate the cavity cross sectional areas in the spanwise direction to arrive at the cavity volume on the blade for a given position of the blade in the wake.

This procedure is repeated at 10^{o} increments of blade rotation, so that the volume history for one blade may be determined over 360^{o} of rotation.

3.0 COMPUTER PROGRAM

All of the calculations necessary to predict the low frequency acoustic radiation from sheet cavitation volume fluctuations are done by a series of interconnected computer programs. Major portions of the current program were adapted from BBN propeller design and analysis programs developed under other contracts.

The program was broken down into distinct modules to simplify programming and debugging. This modular approach also allows portions of the program to be modified as improvements to the theory are made, without affecting other portions of the program.

3.1 Computer Program Organization

As discussed in Ref. 1, the estimation of low frequency acoustic radiation from cavitation volume fluctuations requires four major steps:

1) Select wakefield;

2) Design prop to suit circumferentially averaged wake velocities so that proper thrust or horsepower is obtained;

3) Analyze prop in non-uniform wakefield and determine the volume of cavitation for each position of the blade in the wake;

4) Resolve the cavitation volume vs time history into a Fourier series and compute the farfield radiation at blade rate and harmonics of blade rate.

The computer program has been broken into modules along these same lines, as shown in Fig. 3.1. Each of the major sections of the program are run independently, using data files to effect the transfer of information between sections.

MERCHANT SHIP PROPELLER PROGRAMS - MSP²

FUNCTIONAL BLOCK DIAGRAM

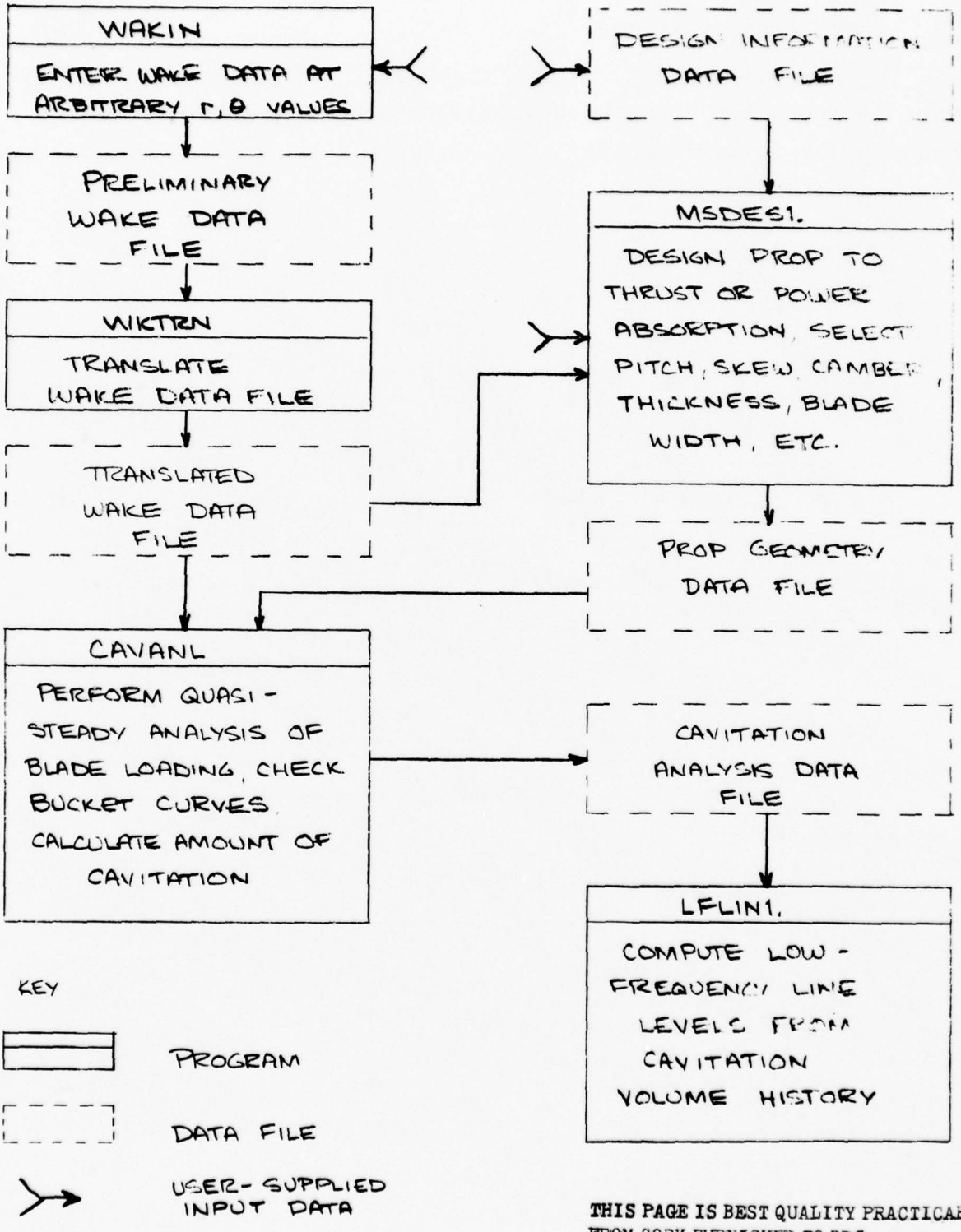

FIGURE 3.1

3.2 Example Computer Run

The computer output showing the design and analysis of the baseline propeller from the sensitivity analysis (Section 6.2) is shown on the following pages, Fig. 3.2.

SAMPLE COMPUTER OUTPUT - DESIGN AND ANALYSIS OF BASELINE PROPELLER FOR SENSITIVITY ANALYSIS (SECTION 6.2).

USER RESPONSES ARE UNDERLINED


```
@TYPE SAPDI1.DAT

;   <DGREELEY>SAPDI1.DAT;1    TUE 20-JUN-78 5:20PM        PAGE 1


0,0.007,0,.5,5768,8,0.2,1.27908E-5,1
0,1,30,50,86,30000,16,1.9905,5
1,1,1,-2,0,0,0,0,0,0
0,0,0,0,0,0,0,0,0
0,0,0,0,0,0,0,0,0
0,0,0,0,0,0,0,0,0
^L
@
```

← DESIGN INFORMATION DATA FILE

DESIGN PROGRAM

```
RUN MSDES1.SAV

    INPUT TRANSLATED WAKE DATA FILENAME:  TANWK4
    INPUT FILE #: 1 FOR DISK, 5 FOR TERM  1
    INPUT FILENAME- 6 LETTERS OR LESS  SAPDI1
    IF CHANGES, ENTER I,J,VALUE.  TO RUN ENTER 9,9,9   9,9,9
    INPUT EAR, POS.MAX CH.,ROOT CH./MAX CH.  .6,.7,.7
    INPUT T/D AT TIP  .0022

    X          0.200 0.300 0.400 0.500 0.600 0.700 0.800 0.900 1.000
    T/C        0.254 0.198 0.158 0.126 0.100 0.077 0.052 0.033 0.027
    SIG.RAT.   0.109 0.288 0.399 0.495 0.568 0.618 0.597 0.550 0.297
    IS BLADE OK? (1=YES)  0
    IF CHANGES, ENTER I,J,VALUE.  TO RUN ENTER 9,9,9   9,9,9
    INPUT EAR, POS.MAX CH.,ROOT CH./MAX CH.  .6,.7,.75   BASELINE
    INPUT T/D AT TIP  .0022

    X          0.200 0.300 0.400 0.500 0.600 0.700 0.800 0.900 1.000
    T/C        0.235 0.191 0.156 0.127 0.102 0.079 0.053 0.033 0.027
    SIG.RAT.   0.100 0.277 0.395 0.500 0.580 0.633 0.608 0.553 0.298
    IS BLADE OK? (1=YES)  1
    IS FULL OUTPUT PRINT DESIRED (1=YES)  1
^L
```

← TRY DIFFERENT BLADE SHAPES

FIGURE 3.2a

20-JUN-78 17:28 DESIGN CONDITIONS ****** **********

VSHIP(KTS)	16.00	THRUST(LBS)	551243.	CTSI	1.0842E+00
DIAM(FT)	30.00	HORSEPOWER	30000.	CPSI	1.0444E+00
RPM	86.00	SHAFT IMMER.	50.00	CTS	1.0729E+00
NO. BLADES	5.	EXP.AREA RATIO	0.600	CPS	1.1884E+00
EFFICIENCY	0.5409	(1-W(V))	0.607	CTHP	6.4284E-01
P/D (.7R)	0.6325	LAMBDA(MEAN)	0.1215	J(MEAN)	0.3816
KT	0.1664	NACA 66,A=0.8 SECTIONS		KQ	0.0184
BURRILL PARAMETERS:		SIGMA(.7R)	0.582	TAU(.7R)	0.154

WEIGHT OF BLADES(LBS): 112959.0
REYNOLDS NUMBER MULTIPLIER= 1.00000

X	TAN B	TAN BI	GS	DCT	DCP	CLIFT	CDRAG
0.200	0.3448	0.7333	0.000E+00	-0.0005	0.0006	0.0000	0.0070
0.300	0.2669	0.5267	2.342E-02	0.6002	0.4917	0.4602	0.0070
0.400	0.2278	0.4215	2.656E-02	0.9638	0.8573	0.3555	0.0070
0.500	0.2044	0.3571	2.815E-02	1.3156	1.2673	0.2813	0.0070
0.600	0.1889	0.3134	2.824E-02	1.6107	1.6809	0.2245	0.0070
0.700	0.1777	0.2814	2.796E-02	1.8801	2.1200	0.1869	0.0070
0.800	0.1668	0.2550	2.652E-02	2.0510	2.4800	0.1591	0.0070
0.900	0.1583	0.2342	2.219E-02	1.9387	2.5249	0.1352	0.0070
1.000	0.1514	0.2173	0.000E+00	0.0000	0.0000	0.0000	0.0070

X	VA/VS	VT/VS	C/D	T/D	T/C	P/D	MCSKEW(DEG)
0.200	0.345	0.000	0.1997	0.0468	0.2345	0.461	-10.78
0.300	0.400	-0.000	0.2190	0.0418	0.1910	0.496	-8.54
0.400	0.455	-0.000	0.2364	0.0369	0.1560	0.530	-6.52
0.500	0.511	-0.000	0.2511	0.0319	0.1269	0.561	-4.78
0.600	0.567	-0.000	0.2619	0.0266	0.1017	0.591	-2.91
0.700	0.622	-0.000	0.2663	0.0211	0.0791	0.619	-0.97
0.800	0.667	-0.000	0.2595	0.0138	0.0530	0.641	1.21
0.900	0.712	-0.000	0.2272	0.0075	0.0329	0.662	3.50
1.000	0.757	0.000	0.0818	0.0022	0.0269	0.683	5.51

X	CLF/CL	F/C 2D	KC	F/C 3D	AL(NT)	SIGMA	SIGMA RATIO
0.200	1.000	0.02969	1.6082	0.04774	0.0000	6.8611	0.0997
0.300	1.000	0.03638	1.3126	0.04774	1.0050	2.9988	0.2770
0.400	1.000	0.02716	1.0169	0.02761	0.5813	1.6516	0.3952
0.500	1.000	0.02091	1.0004	0.02092	0.4403	1.0352	0.4999
0.600	1.000	0.01631	1.0740	0.01752	0.3687	0.7042	0.5798
0.700	1.000	0.01331	1.1741	0.01562	0.3289	0.5068	0.6327
0.800	1.000	0.01107	1.3592	0.01505	0.3168	0.3803	0.6085
0.900	1.000	0.00924	1.8132	0.01676	0.3528	0.2944	0.5530
1.000	1.000	0.00739	2.2671	0.01676	0.0000	0.2335	0.2977

CREATE PROP GEOMETRY DATA FILE

IF CHANGES, ENTER I,J,VALUE. TO RUN ENTER 9,9,9 66
INPUT PROP GEOMETRY DATA FILE NAME SAPG1
INPUT DESCRIPTIVE HEADER, UP TO 70 CHARACTERS
SA BASELINE PROP
IF CHANGES, ENTER I,J,VALUE. TO RUN ENTER 9,9,9

FIGURE 3.26

RUN PROGRAM CAVANL. TO PERFORM QUASI-STEADY CAVITATION ANALYSIS

```
 INPUT PROP GEOMETRY DATA FILE NAME  SAPG1

 WAKE FILE USED FOR PROP DESIGN = TANWK4

 INPUT TRANSLATED WAKE DATA FILENAME:  TANWK4

 INPUT CHANGES IN ANALYSIS CONDITIONS
 INPUT CHANGE CODE, NEW VALUE:  360,36

 ENTER OUTPUT FILE HEADER(UP TO 65 CHAR)
SA BASELINE PROPELLER
 ENTER CAVITATION ANALYSIS DATA FILE NAME:  SACV1
 THETA=   0.0  TBLAD= 178619.  QBLAD= 512883.
 THETA=  10.0  TBLAD= 172763.  QBLAD= 508368.
 THETA=  20.0  TBLAD= 159038.  QBLAD= 486277.
 THETA=  30.0  TBLAD= 142618.  QBLAD= 453980.
 THETA=  40.0  TBLAD= 128163.  QBLAD= 422101.
 THETA=  50.0  TBLAD= 116900.  QBLAD= 395579.
 THETA=  60.0  TBLAD= 108024.  QBLAD= 373789.
 THETA=  70.0  TBLAD= 10653.   BLAD= 354975.
 THETA=  80.0  TBLAD=  94598.  QBLAD= 338998.
 THETA=  90.0  TBLAD=  89827.  QBLAD= 325956.
 THETA= 100.0  TBLAD=  86504.  QBLAD= 316367.
 THETA= 110.0  TBLAD=  85064.  QBLAD= 311409.
 THETA= 120.0  TBLAD=  86718.  QBLAD= 314241.
 THETA= 130.0  TBLAD=  93141.  QBLAD=329054.
 THETA= 140.0  TBLAD= 104961.  QBLAD= 356807.
 THETA= 150.0  TBLAD= 120210.  QBLAD= 392274.
 THETA= 160.0  TBLAD= 131518.  QBLAD= 417763.
 THETA= 170.0  TBLAD= 132500.  QBLAD= 419987.
 THETA= 180.0  TBLAD= 121492.  QBLAD= 395118.
 THETA= 190.0  TBLAD= 103722.  QBLAD= 352560.
 THETA= 200.0  TBLAD=  86174.  QBLAD= 307433.
 THETA= 210.0  TBLAD=  72933.  QBLAD= 271159.
 THETA= 220.0  TBLAD=  65370.  QBLAD= 249184.
 THETA= 230.0  TBLAD=  62450.  QBLAD= 239828.
 THETA= 240.0  TBLAD=  62622.  QBLAD= 239150.
 THETA= 250.0  TBLAD=  64569.  QBLAD= 243504.
 THETA= 260.0  TBLAD=  67725.  QBLAD= 251209.
 THETA= 270.0  TBLAD=  72320.  QBLAD= 262712.
 THETA= 280.0  TBLAD=  78700.  QBLAD= 278677.
 THETA= 290.0  TBLAD=  87237.  QBLAD= 299760.
 THETA= 300.0  TBLAD=  98480.  QBLAD= 327007.
 THETA= 310.0  TBLAD= 113376.  QBLAD= 362247.
 THETA= 320.0  TBLAD= 131284.  QBLAD= 403067.
 THETA= 330.0  TBLAD= 150149.  QBLAD= 444376.
 THETA= 340.0  TBLAD= 165973.  QBLAD= 478299.
 THETA= 350.0  TBLAD= 176122.  QBLAD= 501971.
```

OUTPUTS THRUST & TORQUE PER BLADE AT EACH θ STEP

FIGURE 3.2c

20-JUN-78 18:05 LOW FREQUENCY LINE CALCULATION
*** ********* **** **********

CAVITATION ANALYSIS DATA FILE: SACV1
SA BASELINE PROPELLER

WAKE DATA FILE: TANWK4
PROP GEOMETRY DATA FILE: SAPG1

VSHIP(KTS)	16.00	DIAM(FT)	30.00	SHAFT IMMER(FT)	50.00
RPM	86.00	NO. BLADES	5	EXP. AREA RATIO	0.600
THRUST	543405.	KT	0.1641	SIGMA(VS)	7.271
DHP	29424.	10*KQ	0.1808	SIGMA(N)	2.872

VALUES FOR INDEX BLADE:

THETA DEG	CAVITY AREA (FT**2)	AC/AB	CAVITY VOLUME (FT**3)	
0.00	8.59	0.105	0.54685	BACK CAVITATION
10.00	9.28	0.114	0.50992	
20.00	2.37	0.029	0.06488	
30.00	0.36	0.004	0.00221	
40.00	0.00	0.000	0.00000	
50.00	0.00	0.000	0.00000	
60.00	0.00	0.000	0.00000	
70.00	0.00	0.000	0.00000	
80.00	0.00	0.000	0.00000	
90.00	0.00	0.000	0.00000	
100.00	0.00	0.000	0.00000	
110.00	0.00	0.000	0.00000	
120.00	0.00	0.000	0.00000	
130.00	0.00	0.000	0.00000	
140.00	0.00	0.000	0.00000	
150.00	0.00	0.000	0.00000	
160.00	0.00	0.000	0.00000	
170.00	0.00	0.000	0.00000	
180.00	0.00	0.000	0.00000	
190.00	0.00	0.000	0.00000	
200.00	0.00	0.000	0.00000	
210.00	0.00	0.000	0.00000	
220.00	0.00	0.000	0.00000	
230.00	0.00	0.000	0.00000	
240.00	0.30	0.004	0.00239	FACE CAVITATION
250.00	0.31	0.004	0.00239	
260.00	0.13	0.002	0.00082	
270.00	0.14	0.002	0.00082	
280.00	0.00	0.000	0.00000	
290.00	0.00	0.000	0.00000	
300.00	0.00	0.000	0.00000	
310.00	0.00	0.000	0.00000	
320.00	0.00	0.000	0.00000	
330.00	0.79	0.010	0.01052	BACK CAVITATION
340.00	3.79	0.047	0.14180	
350.00	7.59	0.093	0.41666	

AVERAGE CAVITY VOLUME (FT**3): 0.23654 (FOR WHOLE PROPELLER)

FIGURE 3.2d

SACV1
BASELINE PROPELLER

LINE LEVEL CALCULATIONS: HARMONICS OF BLADE RATE
ACOUSTIC PRESSURES IN DB RE 1MICROPASCAL AT 1YARD

N	FREQ (HZ)	A(N) (FT**3)	MONOPOLE SPL(DB)	LLOYD MIRROR(DB)	LRESL (DB)	MONOPOLE @30 FT(DB)
1	7.17	0.299664	180.7	-20.4	160.3	185.2
2	14.33	0.058664	178.6	-14.5	164.2	183.1
3	21.50	0.033294	180.7	-11.0	169.7	185.2
4	28.67	0.015400	179.0	-8.6	170.5	183.5
5	35.83	0.003401	169.8	-6.7	163.1	174.2
6	43.00	0.002303	169.6	-5.3	164.3	174.0
7	50.17	0.000448	158.0	-4.1	153.9	162.5
8	57.33	0.000594	162.8	-3.1	159.7	167.3
9	64.50	0.000846	167.9	-2.3	165.6	172.4
10	71.67	0.001235	173.0	-1.6	171.4	177.5

LONG RANGE [illegible]
SOURCE LEVEL

END OF EXECUTION

MONOPOLE
SOURCE STRENGTH
AT SHAFT CENTERLINE

FIGURE 3.2e

4.0 EXAMPLE CALCULATIONS USING MERCHANT SHIP PROPELLER PROGRAM

Several examples of calculations done using the current computer programs are presented in this section to illustrate the accuracy and the shortcomings of the program.

4.1 Calculated and Observed Cavitation Patterns

4.1.1 Single screw merchant ship

The first example is taken from ref. 14 and deals with the propeller for a medium size single screw cargo vessel, with the following particulars:

Ship speed = 15.8 knots
Prop diameter = 15.9 feet
RPM = 155.5
Shaft horsepower = 9500
No. of blades = 4
Expanded Area Ratio = 0.6 (ratio of blade area to propeller disc area)

The cavitation properties of this propeller were determined by running a model in a cavitation tunnel in a simulated ship wake-field. The results of the cavitation tunnel tests are shown in Fig. 4.1, along with the predictions computed in ref. 14 and the BBN predictions using the current computer programs.

Van Cassanen's predicted cavitation patterns come much closer to matching the observed cavitation patterns. Note, however, that van Oossanen's predictions are for the model propeller while the BBN predictions are for the full scale propeller. Reference 14 points out that the large Reynolds number difference between model and full scale propellers can have considerable impact on the cavitation patterns experienced under otherwise identical flow conditions. The theory developed by van Oossanen in ref. 14 goes to

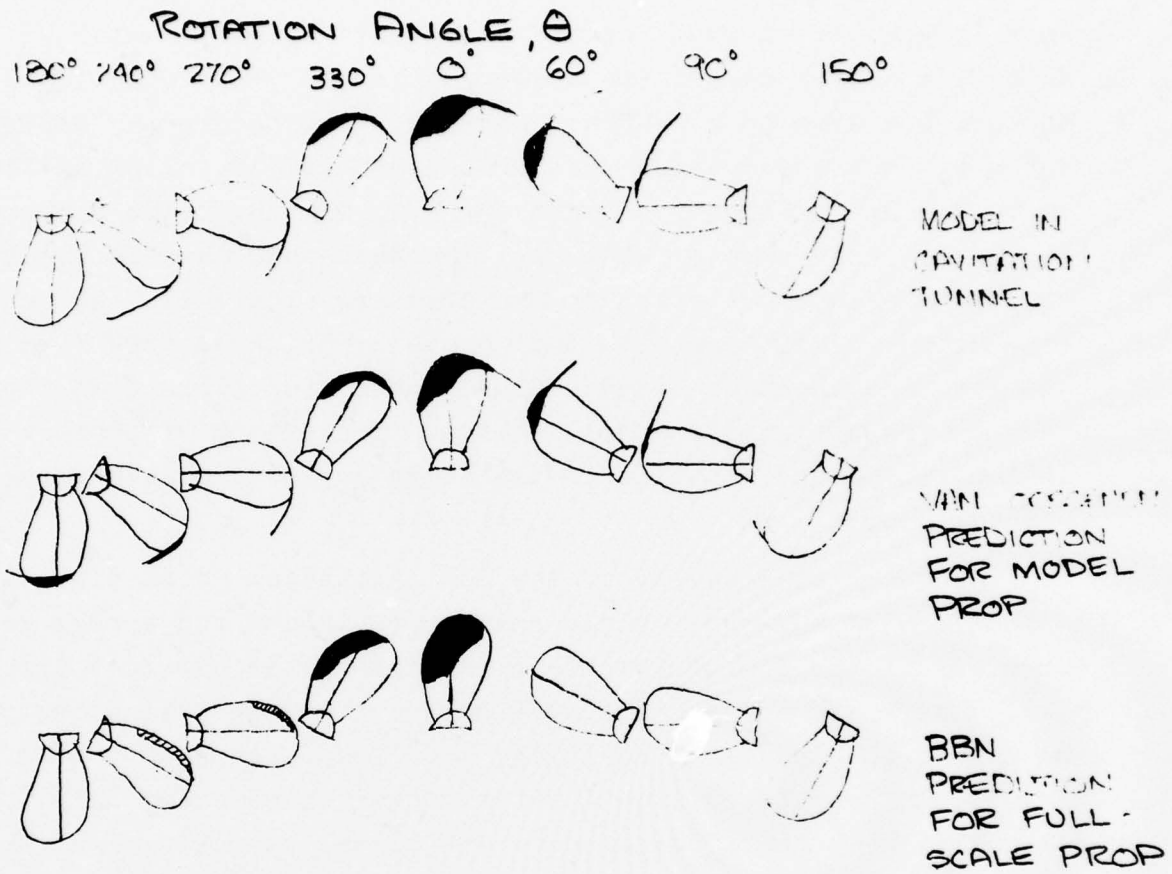

FIGURE 4.1 COMPARISON OF CALCULATED & OBSERVED CAVITATION PATTERNS - SINGLE SCREW MERCHANT SHIP

great lengths to account for the effect of Reynolds number on cavitation, which causes the theory to be much more complicated than the one developed by BBN. However, both theory and experiment show that the methods used in the BBN cavitation prediction scheme are approximately correct for very high Reynolds numbers; i.e., full scale ship propellers. The fact that the BBN prediction shows sheet cavitation on the pressure side while the model tests do not is in line with full scale experience: this form of cavitation has been observed on full scale propellers even though none was present during model testing. The extent of sheet cavitation on the suction side of the blade may also change with Reynolds number.

The major shortcoming of the BBN cavitation prediction scheme is the lack of a way to handle cavitation in the tip vortex which comes off of the tip of the blade (similar to an aircraft tip vortex). There are as yet no simple methods for predicting the volume and extent of tip vortex cavities, but it appears that the cavitation volume associated with the tip vortex on merchant ship propellers will be small compared to the volume resulting from sheet cavitation. Hence the tip vortex cavitation volume may influence the generation of noise at the higher harmonics of blade rate, but probably won't affect the acoustic radiation at the lower harmonics, which are of primary interest in the present work.

4.1.2 Twin screw merchant ship

The second example is also taken from van Oossanen's work (ref. 14) and concerns the propeller of a fast twin screw vessel with the following particulars:

Design ship speed = 30 knots
Prop diameter = 11.98 feet
Design RPM = 230

Design horsepower = 15500
No. of blades = 5
Expanded Area Ratio = 0.8

The observations and predictions shown in Fig. 4.2 are for a ship speed of 24 knots, with the prop turning at 176 RPM. It is seen that the correlation between full scale observations and the BBN prediction is satisfactory, with the exception of the tip vortex cavity.

It is interesting to note that a model test of the same propeller under identical flow conditions (except for the smaller Reynolds number associated with the model) did not show any evidence of sheet cavitation on the pressure side of the blade, as is shown in Fig. 4.2 (283^{o} and 312^{o} positions). This reinforces the discussion in Section 4.1.1 concerning Reynolds number effects on cavitation patterns.

4.2 Shortcomings of Prediction Process

It appears that the major problem with the BBN cavity prediction process is the neglect of the tip vortex cavity. As noted previously, neglecting this phenomenon will probably only affect the radiated noise at the higher harmonics of blade rate, so that it would appear to be safe to neglect this in the current work which is mainly concerned with correctly modelling the first few harmonics of blade rate. The effect of the tip vortex cavity will be included as soon as time and funds permit.

A brief note on the whole concept of mathematically modelling propeller cavitation is in order here. Although it is clear that the prediction process is subject to continual improvement and refinement, there is a danger that the associated calculations can get so complicated and expensive, and require so much input data, that they are of little use in solving the problem at hand

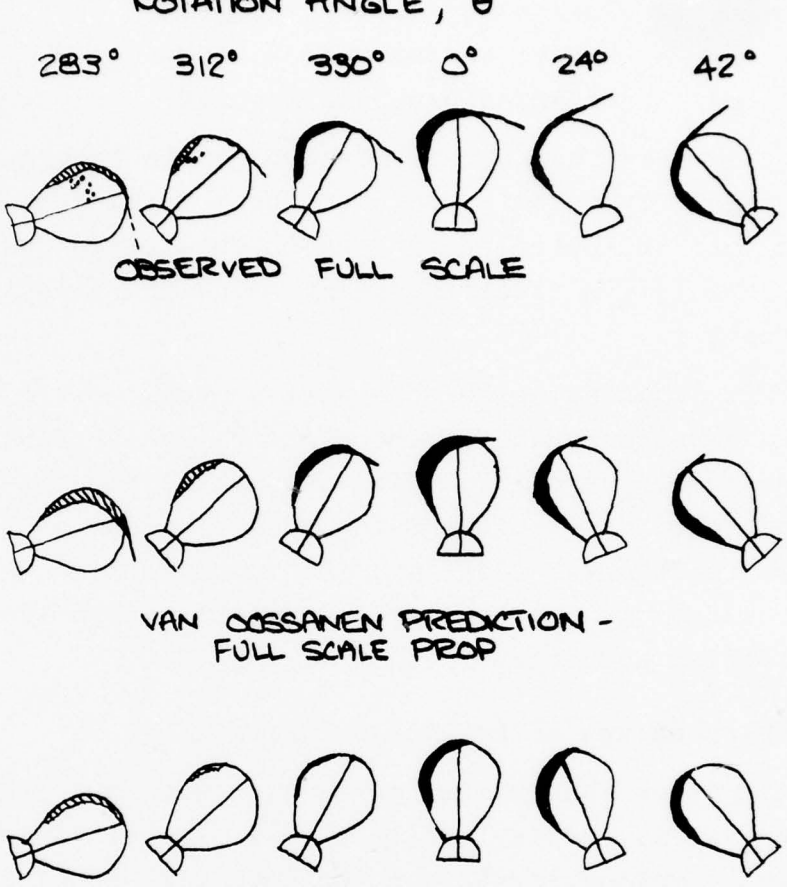

FIGURE 4.2 COMPARISON OF CALCULATED & OBSERVED CAVITATION PATTERNS - TWIN SCREW MERCHANT VESSEL

(predicting ocean ambient noise). We believe that the present model is probably adequate for predicting radiated noise at the first few harmonics of blade rate but will require some improvements, such as including the tip vortex cavity, before it is useful for predicting the cavitation noise at the higher harmonics of blade rate.

Further comparisons (beyond the two presented here) of predicted cavitation patterns with those measured on full scale propellers should be conducted before exercising this program to predict the ensemble characteristics of ocean ambient noise due to merchant ship propeller cavitation. These comparisons are necessary in order to establish whether or not the current program provides unbiased estimates of propeller cavitation volume.

5.0 REVIEW OF LINE LEVEL PREDICTION PROCESS

5.1 Radiation from Cavitation Volume Fluctuations

For the purposes of calculating acoustic radiation, the present work assumes that the sheet cavitation volume fluctuations may be adequately represented by an equivalent monopole at an appropriate depth below the surface (currently assumed to be at the propeller shaft centerline). Then the pressure radiated from this simple volume source is:

$$\langle p^2 \rangle = \langle Q^2 \rangle \left(\frac{f\rho}{2r} \right)^2 \tag{5.1}$$

where $\langle p^2 \rangle$ = mean square pressure

$\dot{Q}$ = volume velocity

f = frequency (Hz)

r = radius from acoustic enter

ρ = density of fluid

If we represent the cavitation volume history for the whole propeller as a Fourier series

$$Q(t) = \sum_{N=0}^{\infty} A_N e^{iN\omega t} \tag{5.2}$$

where Q(t) = cavitation volume on prop

A_N = complex coefficient

N = harmonic number

ω = blade rate frequency (rad/sec) = $\frac{\text{RPM prop}}{60} \cdot 2\pi B$

B = number of propeller blades

then

$$\dot{Q}(t) = \sum_{N=0}^{\infty} N\omega A_N e^{iN\omega t} \tag{5.3}$$

and $$\langle \dot{Q}^2 \rangle = \frac{1}{2} \sum_{N=0}^{\infty} N^2 \omega^2 |A_N|^2 \tag{5.4}$$

Therefore the radiated pressure at the N-th harmonic of blade rate is

$$\langle p^2 \rangle = \frac{N^2 \omega^2 |A_N|^2}{2} \cdot \left(\frac{f_N \rho}{2r} \right)^2 \tag{5.5}$$

The frequency f_N of the N-th harmonic of blade rate is

$$f_N = \frac{N\omega}{2\pi} \tag{5.6}$$

So that Eq. 5.5 reduces to

$$\langle p^2 \rangle = 2\pi^2 f_N^2 |A_N|^2 \left(\frac{f_N}{2} \frac{\rho}{r} \right)^2$$

$$= \frac{\pi^2 f_N^4 |A_N|^2 \rho^2}{2 r^2} \cdot \tag{5.7}$$

The problem of predicting the cavitation line spectrum at blade rate and harmonics thus consists of finding the coefficients A_N in Fourier series expansion of the propeller cavitation volume history.

The coefficients A_N may be determined from the volume history of a single propeller blade, as shown below. Representating the cavitation volume on the first (index) blade as a Fourier series expansion in rotation angle $\theta (0<\theta<2\pi)$

$$V_1(\theta) = \sum_{n=0}^{\infty} C_n e^{in\theta} \tag{5.8}$$

where C_n = complex coefficient

and assuming all of the blades have identical volume histories, the volume on the bth blade will be

$$V_b(\theta) = V_1 \left(\theta + \frac{(b-1)2\pi}{B} \right)$$

and the volume history for the whole propeller will be

$$V_p(\theta) = \sum_{n=0}^{\infty} \sum_{b=1}^{B} C_n e^{in(\theta+\frac{2\pi b}{B})}$$

$$= \sum_{n=0}^{\infty} C_n e^{in\theta} \cdot \sum_{b=1}^{B} e^{in\frac{2\pi b}{B}} \qquad (5.9)$$

The first summation above is the volume history of the index blade $[V_1(\theta)]$ and the second summation has nonzero values only for values of n equal to integer multiples of B, i.e.,

$$\sum_{b=1}^{B} e^{in\frac{2\pi b}{B}} = \begin{cases} B, & n=k\cdot B \\ 0, & n\neq k\cdot B \end{cases} \qquad (5.10)$$

Thus the cavitation volume history on a cavitating propeller with B blades, in terms of the Fourier series expansion coefficients for the volume history on the index blade, C_n, is

$$V_p(\theta) = B \sum_{k=0}^{\infty} C_{B\cdot K} e^{i(Bk\theta)} \qquad (5.11)$$

Since rotation angle θ and time t are directly related by the rotational speed of the propeller, with the period of rotation T corresponding to 2π radians of rotation, we may write

$$V_p(t) = B \sum_{k=0}^{\infty} C_{B\cdot k} e^{i\frac{2\pi Bk}{T}t} \qquad (5.12)$$

Comparing equations (5.2) and (5.12), we see that $Q(t) \equiv V_p(t)$, so that

$$\sum_{N=0}^{\infty} A_N e^{iN\omega t} = B \sum_{k=0}^{\infty} C_{B\cdot k}\, e^{i\frac{2\pi Bk}{T}t} \qquad (5.13)$$

Changing the index of summation k to N on the right hand side, and noting that $\frac{2\pi B}{T} = \omega$ (blade rate frequency), we obtain

$$\sum_{N=0}^{\infty} A_N e^{i\omega Nt} = B \sum_{N=0}^{\infty} C_{B\cdot N}\, e^{i\omega Nt},$$

so $$A_N = B\cdot C_{B\cdot N}$$

or

$$|A_N| = B\cdot|C_{B\cdot N}| \qquad (5.14)$$

Thus to get the radiated acoustic pressure at the Nth harmonic of blade rate, we must compute the (B·N)th harmonic of the index blade cavitation volume history.

This immediately causes problems in predicting the radiated noise at higher harmonics of blade rate, since high harmonics of the index blade volume history are required. Although the magnitude of these higher harmonics will be small, equation (5.7) shows that

$$\langle p^2\rangle \sim f_N^{\,4}|A_N|^2$$

so that the $f_N^{\,4}$ term will cause the higher harmonics (up to about 7th and possibly beyond) to radiate significant power.

5.3 Method of Calculating A_N

The current computer program calculates the cavitation volume on the index blade at evenly spaced values of θ. The choice of

the spacing is a compromise between two opposing considerations: computer costs and accuracy. For this sensitivity analysis, most of the computations have been done using 10° increments of θ, yielding 36 data points ($360^{\circ}/10^{\circ} = 36$). If we were to do a harmonic analysis on only these 36 original points, then we could calculate only the first 18 harmonics *at most* (Nyquist frequency). For a 5 bladed propeller, Eq. (5.14) tells us that we could then compute the radiated noise only up to the third harmonic ($|A_3| = 5\ |C_{15}|$). Furthermore, since there may be frequency content beyond twice the folding frequency, there may be aliasing even below the Nyquist frequency.

To attempt to alleviate some of the aliasing problems, the computer program is set up to pass a "smooth" curve (continuous first derivative) through the calculated points and interpolate additional points (for a total of 240 points) before performing the harmonic analysis. Obviously, this procedure is only as valid as the assumption that the growth and collapse of the sheet cavitation bubble is a "smooth" process. This points is discussed further in Section 6.4.

6.0 SENSITIVITY ANALYSIS

6.1 Purpose

The purpose of this sensitivity analysis is to determine the influence of analysis parameters, propeller characteristics, and wakefield characteristics on the prediction of cavitation line spectra. This will provide guidance in improving the prediction procedure and suggest which factors are important in influencing the cavitation noise from merchant ships. It is these factors which must be determined for the world's merchant ship fleet in order to estimate the ensemble characteristics of the ocean ambient noise due to merchant ship propeller cavitation.

6.2 Baseline Propeller and Wakefield

The baseline propeller for this sensitivity analysis is similar to a propeller which might be found on a 300,000 deadweight ton tanker. The wakefield for such a ship was estimated from the data presented in Ref. 17, and is shown in Figures 6.1 and 6.2. The baseline propeller was designed to match this wake and has the following characteristics:

Diameter = 30.0 ft
Design RPM = 86
Design ship speed - 16.0 knots
Horsepower at design speed = 30,000 SHP
Number of blades = 5
Expanded Area Ratio = 0.6
Percentage of lift by camber = 100%
Immersion to shaft ℄ = 50.0 ft
Optimum pitch distribution
(maximum efficiency)
B-Series skew distribution
Blade thickness based on strength criteria

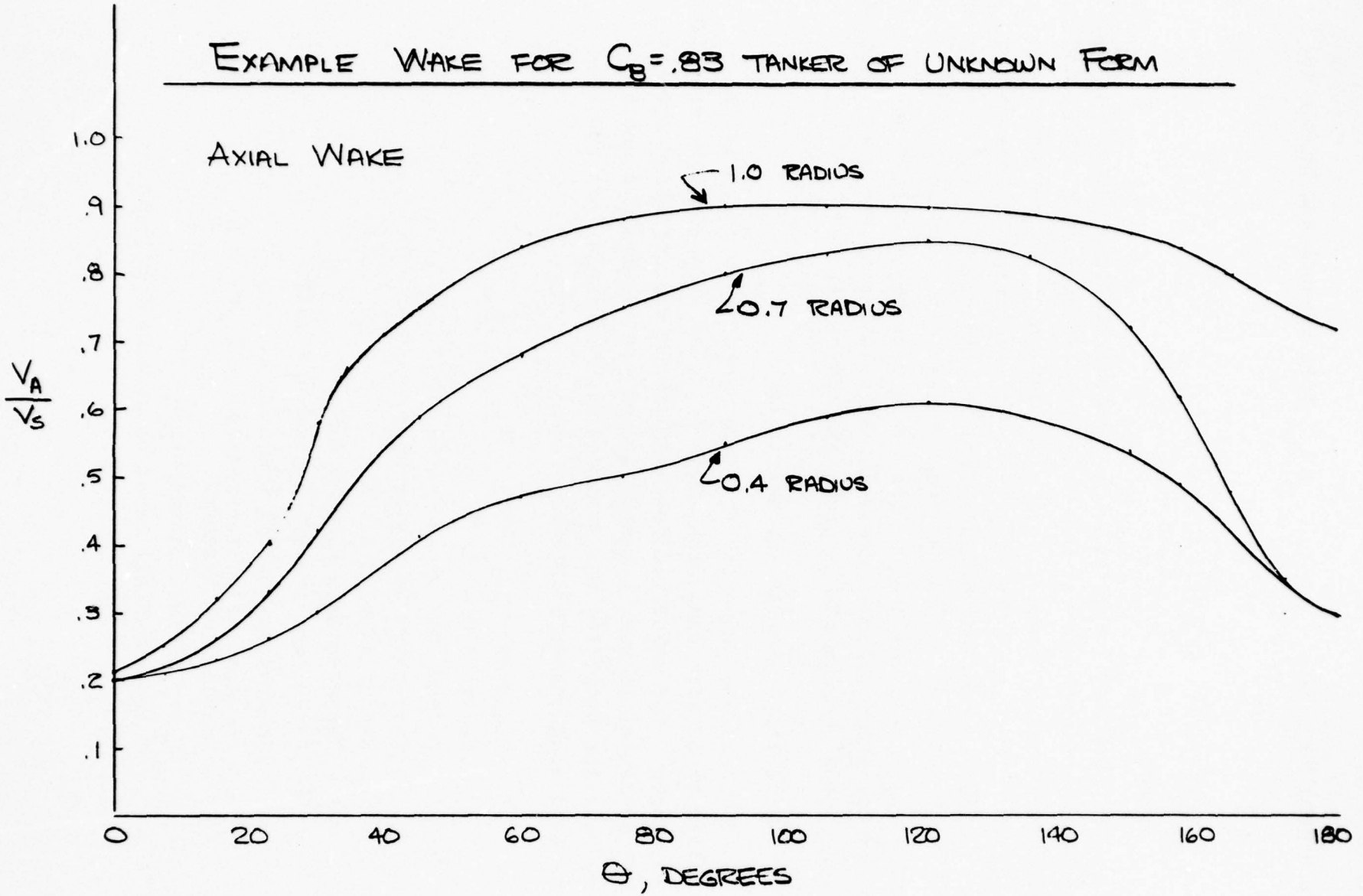
EXAMPLE WAKE FOR C_B=.83 TANKER OF UNKNOWN FORM
AXIAL WAKE
1.0 RADIUS
0.7 RADIUS
0.4 RADIUS
$\frac{V_A}{V_S}$
1.0
.9
.8
.7
.6
.5
.4
.3
.2
.1
0
20
40
60
80
100
120
140
160
180
Θ, DEGREES

FIGURE 6.1

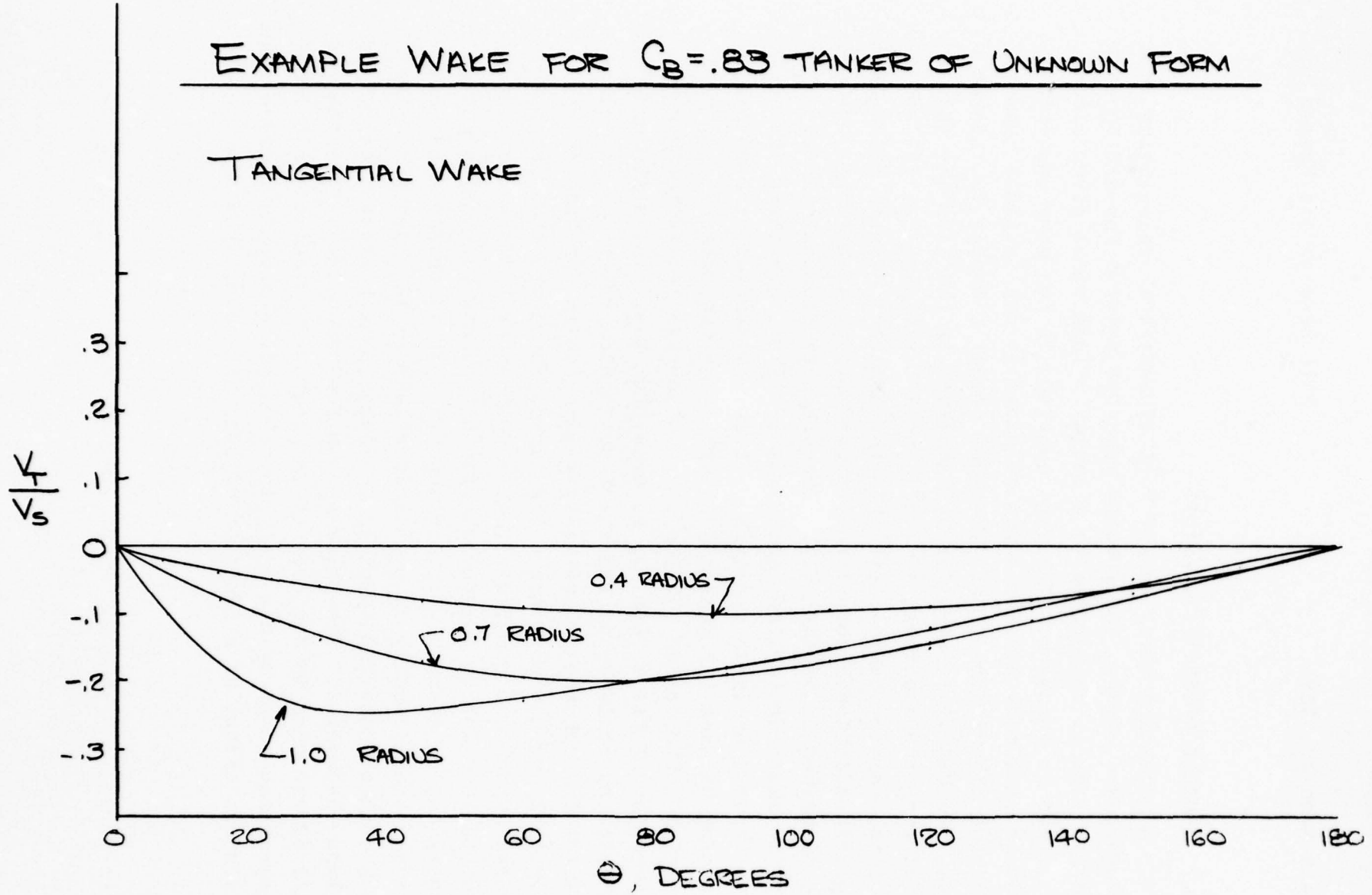
EXAMPLE WAKE FOR C_B=.83 TANKER OF UNKNOWN FORM
TANGENTIAL WAKE
$\frac{V_T}{V_S}$
.3
.2
.1
0
-.1
-.2
-.3
0.4 RADIUS
0.7 RADIUS
1.0 RADIUS
0
20
40
60
80
100
120
140
160
180
Θ, DEGREES

FIGURE 6.2

6.3 Number of Analysis Points

A necessary check on any sort of numerical calculation is a convergence check. The present computer program appears to have no problems in converging to a cavity volume for a given blade position in the wake. The real question is how many analysis points (how many θ values) are required to get reliable results for the higher harmonics. In order to get a handle on this problem, the baseline propeller was analyzed in the baseline wake for 3 different θ spacings: 10^{o}, 5^{o}, and 3^{o}, yielding 36, 72, and 120 points, respectively. Note that the computer program still interpolates additional points before performing the harmonic analysis, as described in Section 5.3. The predicted monopole source levels at the shaft centerline, in dB//(1 μPa$\times$YD)^{2}, are shown in Fig. 6.3 for these 3 analysis spacings. It is obvious that the analysis spacing becomes increasingly important as the harmonic number increases. The reason for the large discrepancies at the higher harmonics of blade rate may be seen from Fig. 6.4, which show the growth and collapse of the sheet cavitation volume as the blade passes through the low velocity region behind the ship in the vertical upright position. The curves shown are the "smooth" curves which the computer program passes through the calculated points in order to interpolate further points for the harmonic analysis, as described in Section 5.3. It is obvious that relatively small spacing of points is necessary in order to define all of the lumps and bumps in the curve, which greatly affect the higher harmonics. The major reason for not using a fine spacing all of the time is the cost of the computer calculations. The approximate cost of the analysis for a given prop in a given wake is shown below, as a function of analysis point spacing:

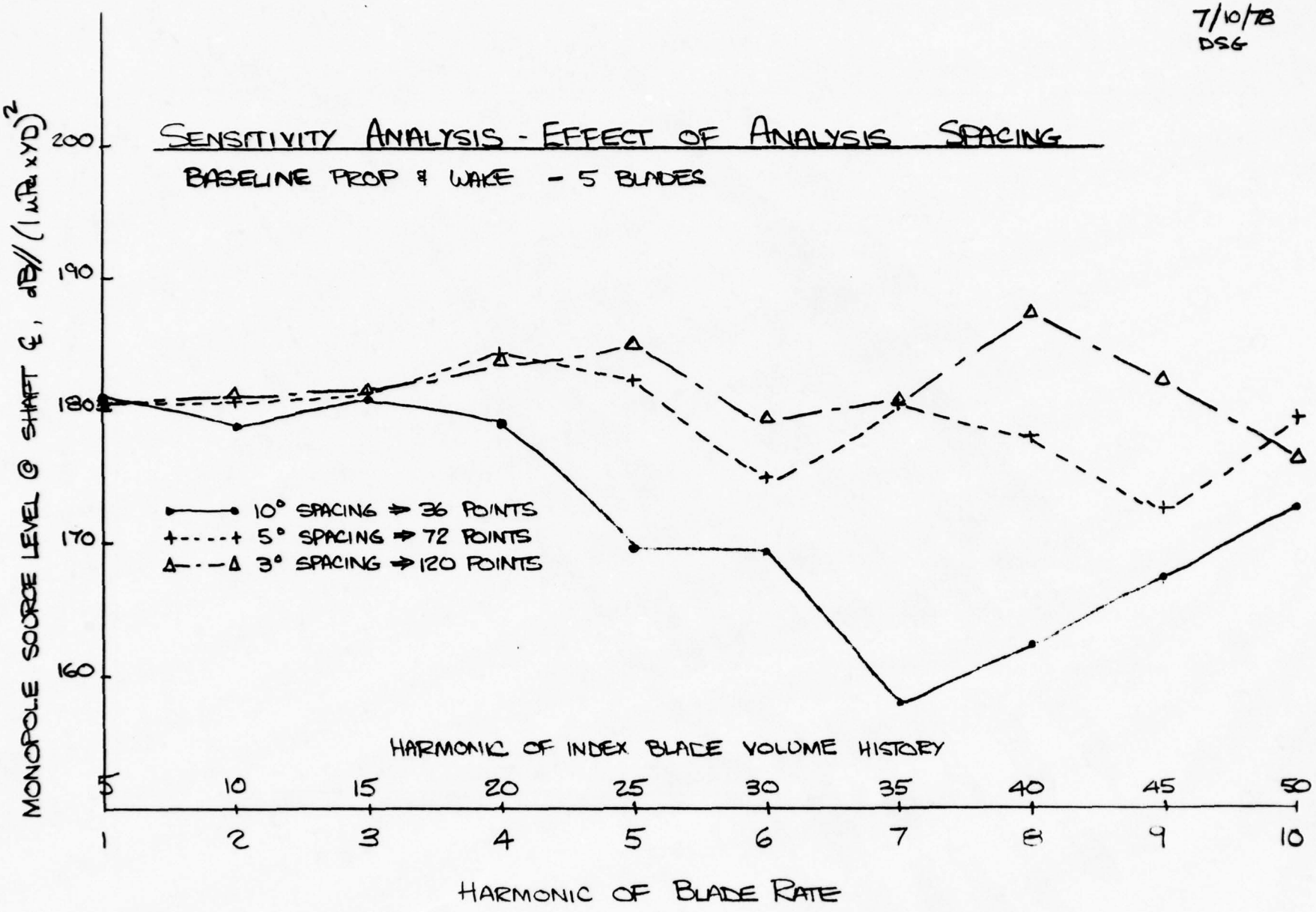
7/10/78
DSG
SENSITIVITY ANALYSIS - EFFECT OF ANALYSIS SPACING
BASELINE PROP & WAKE - 5 BLADES
MONOPOLE SOURCE LEVEL @ SHAFT ℄, dB// (1 μPa x YD)²
200
190
180
170
160
10° SPACING ⇒ 36 POINTS
5° SPACING ⇒ 72 POINTS
3° SPACING ⇒ 120 POINTS
HARMONIC OF INDEX BLADE VOLUME HISTORY
5
10
15
20
25
30
35
40
45
50
1
2
3
4
5
6
7
8
9
10
HARMONIC OF BLADE RATE

FIGURE 6.3

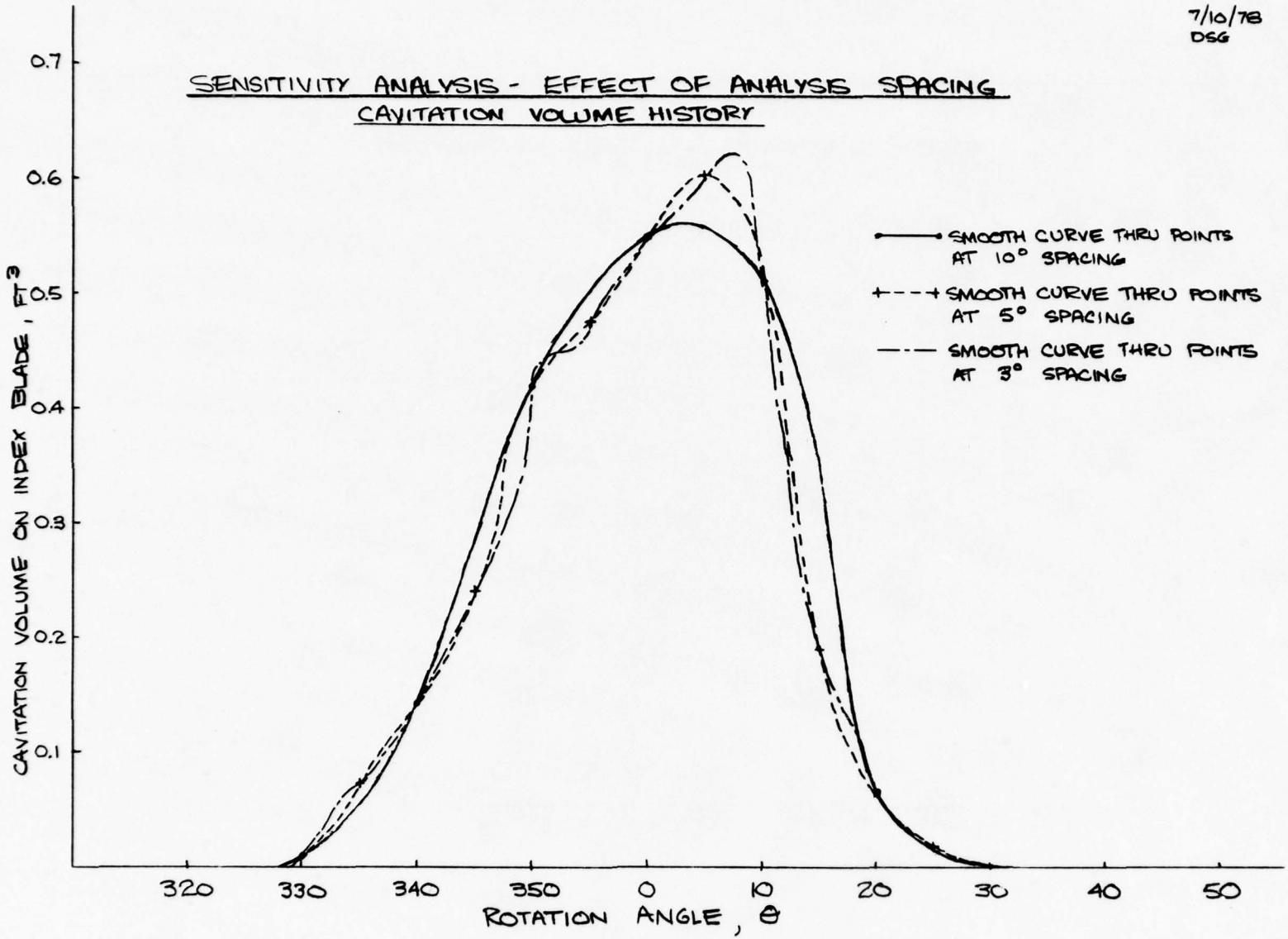
7/10/78
DSG
SENSITIVITY ANALYSIS - EFFECT OF ANALYSIS SPACING
CAVITATION VOLUME HISTORY
SMOOTH CURVE THRU POINTS AT 10° SPACING
SMOOTH CURVE THRU POINTS AT 5° SPACING
SMOOTH CURVE THRU POINTS AT 3° SPACING
CAVITATION VOLUME ON INDEX BLADE, FT³
0.7
0.6
0.5
0.4
0.3
0.2
0.1
320
330
340
350
0
10
20
30
40
50
ROTATION ANGLE, θ

FIGURE 6.4

Analysis Spacing	Number of Points	Approx Cost
10^o	36	\$14
5^o	72	\$27
3^o	120	\$45

While these costs are reasonable, it is obvious that the total bill can become substantial if many propellers are analyzed with a very small spacing. Since it is not yet clear that the higher harmonics may be accurately calculated without some consideration of bubble dynamics and the tip vortex cavity, the sensitivity analysis presented here was done using 10^o analysis spacing for the most part. Only the first, second, and third harmonics of blade rate will be reported for the majority of the cases.

6.4 Generation of Higher Harmonics

In deciding whether or not the quasi-steady type of cavitation analysis used in the present work is really useful in predicting the cavitation noise at higher harmonics of blade rate, it is necessary to determine the cause of these higher harmonics. There are three major possible causes; two physical and one related to numerical analysis problems. These are listed below.

- The response (change in loading) of the propeller blade to the higher harmonics of the wakefield.
- The non-linearities and threshold phenomena present in the cavitation process (non-linear response of a system to a sinusoidal input will generate harmonics).
- The discretization of the blade when calculating the cavitation volume present.

In order to see which of these phenomenae are important, the baseline propeller was analyzed in a perfectly sinusoidal wakefield (once per revolution sinusoidal variation in inflow velocity). The resulting predicted source levels at the various harmonics of blade rate are shown in Fig. 6.5 It is clear that response of the blade to higher harmonics of the inflow perturbations is not necessary to generate high harmonics, and implies that the response of the blade need only be calculated for the first few harmonics of the inflow perturbations. This is very encouraging, since the quasi-steady lifting line theory used in the present computer program is perfectly adequate for performing these calculations. If the response of the blade to the higher harmonics at the inflow perturbations were required, a far more complicated unsteady lifting surface theory would be needed to correctly calculate the response of the blade to inflow perturbations.

A look at the actual volume vs θ history for this propeller (Fig. 6.6) is quite revealing. The jumps in the volume at θ values of approximately 310° and 30° are indeed due to numerical discretization errors. These arise because the cavity cross sectional areas which are integrated in the radial direction to calculate cavity volume are calculated only at a finite number of radial positions on the blade. The sudden jump in the calculated volume is due to a sudden calculated jump in the radial extent of cavitation. In reality, though, the radial extent of the sheet cavitation bubble will *tend* to vary smoothly. Hence this sudden jump is mostly a problem associated with the numerical procedure used. These jumps or discontinuities in the volume history will contribute to the higher harmonics.

Note, however, that even if the discontinuities mentioned above were not present in Fig. 6.6, there would still be significant higher harmonic content. This may be illustrated as follows.

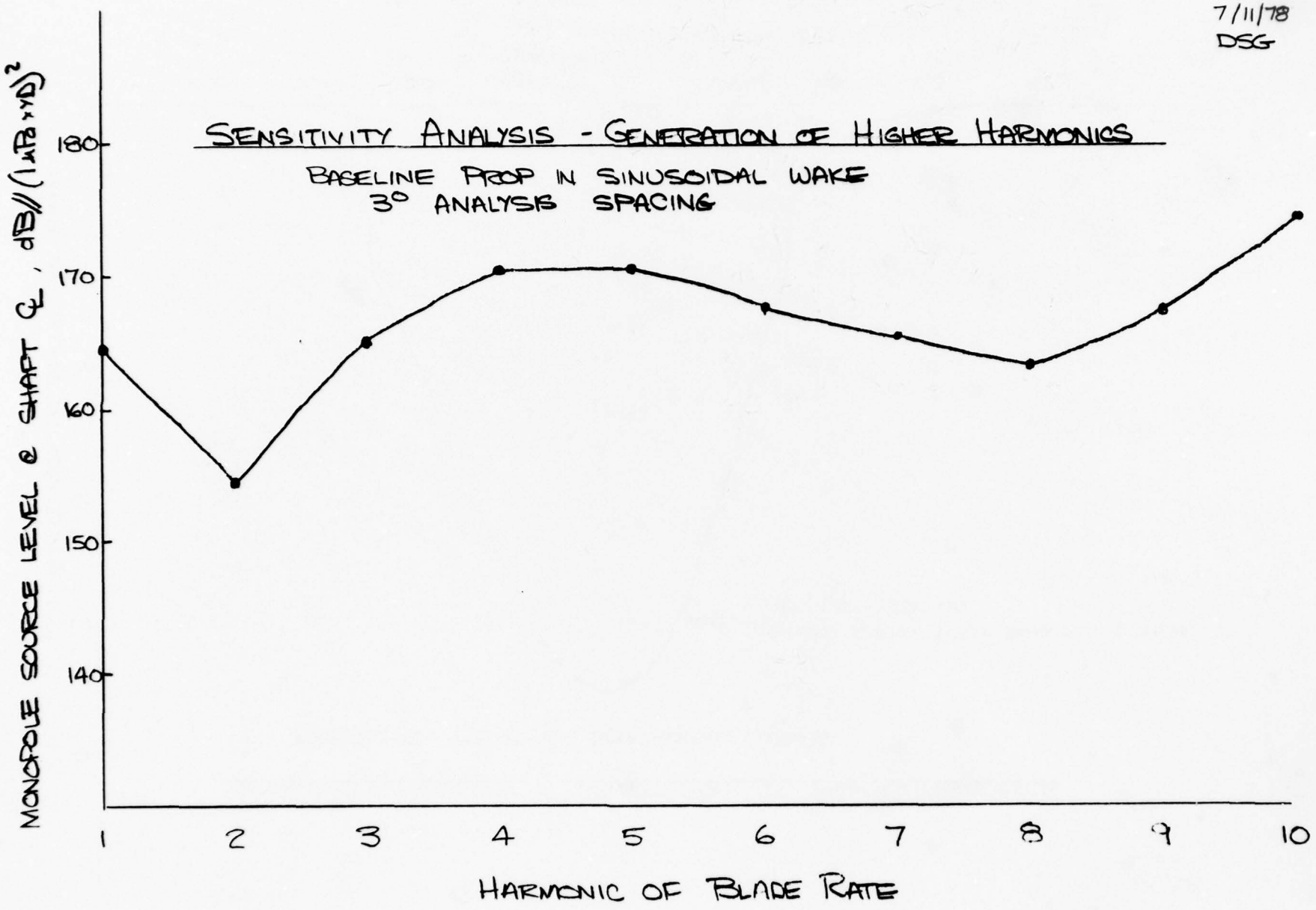
7/11/78
DSG
SENSITIVITY ANALYSIS - GENERATION OF HIGHER HARMONICS
BASELINE PROP IN SINUSOIDAL WAKE
3° ANALYSIS SPACING
MONOPOLE SOURCE LEVEL @ SHAFT ℄, dB// (1 μPa, yD)²
180
170
160
150
140
1
2
3
4
5
6
7
8
9
10
HARMONIC OF BLADE RATE

FIGURE 6.5

7/11/78
DSG

FIGURE 6.6

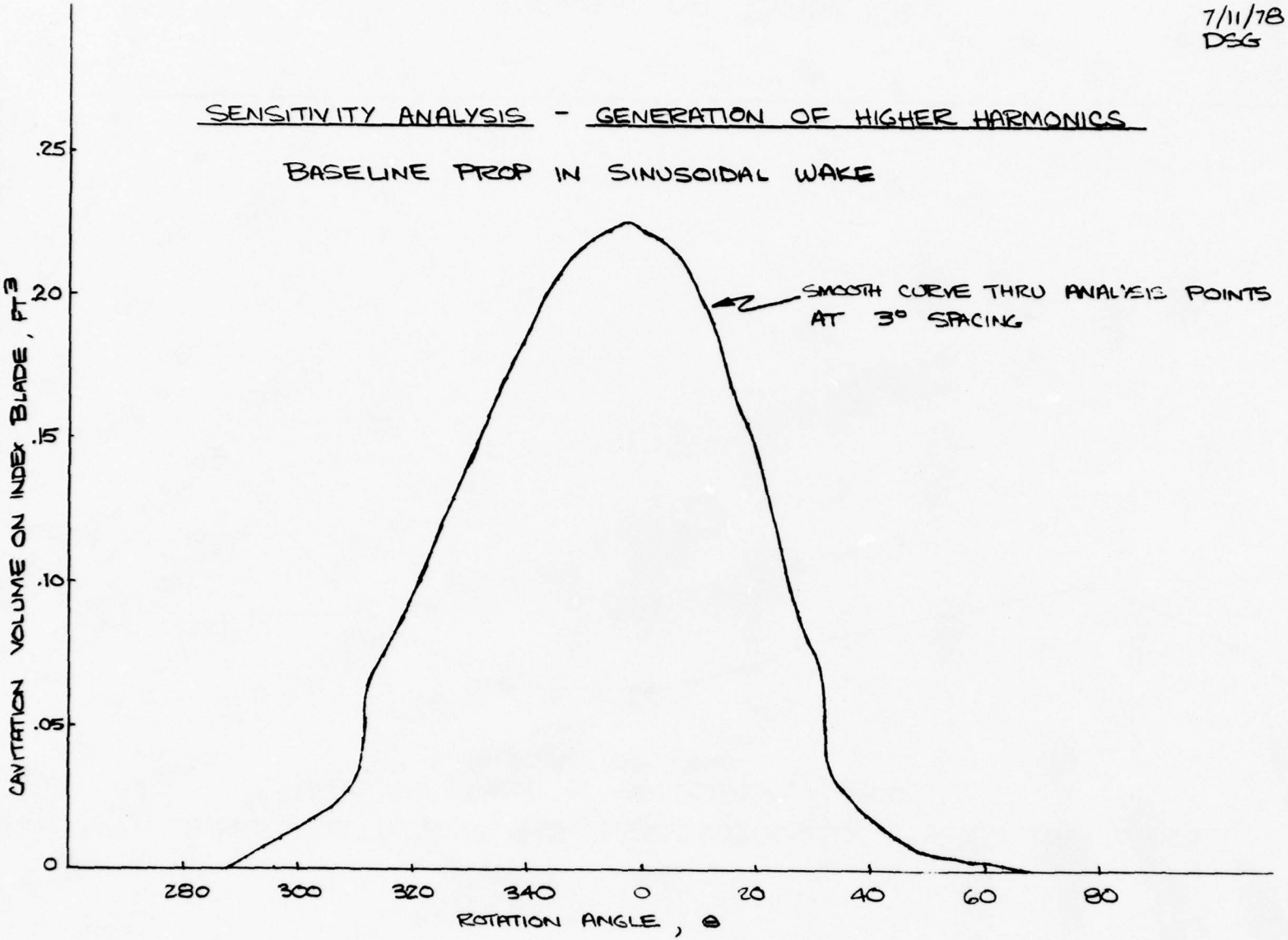

The calculated volume history may be represented (at least to first order) by a triangular shape, as shown in Fig. 6.7. To get the resulting frequency content, we take the Fourier transform of this triangular distribution, which is

$$F(\omega) = \tau \frac{\sin^2 \frac{\omega\tau}{2}}{\frac{\omega\tau}{2}^2} \qquad (6.1)$$

A graph of amplitude ($F(\omega)$) vs frequency (ω) for this function will obviously have nulls because of the $\sin^2$ term. However, if we restrict our attention only to the upper *envelope* of the function and concern ourselves only with the dependence on frequency (in order to bound the problem), we may write

$$F(\omega) \sim \frac{1}{\omega^2} \qquad (6.2)$$

Referring to the radiation relationships developed in Section 5.1, we see that for an observer at a constant distance from a volume source

$$\langle p^2 \rangle \sim f_N^4 |A_N|^2 \qquad (6.3)$$

(from Eq. (5.7))

Noting that

$$f_N \sim \omega$$

and

$$|A_N| \sim F(\omega)$$

then substituting into Equation 6.3 yields

7/11/78

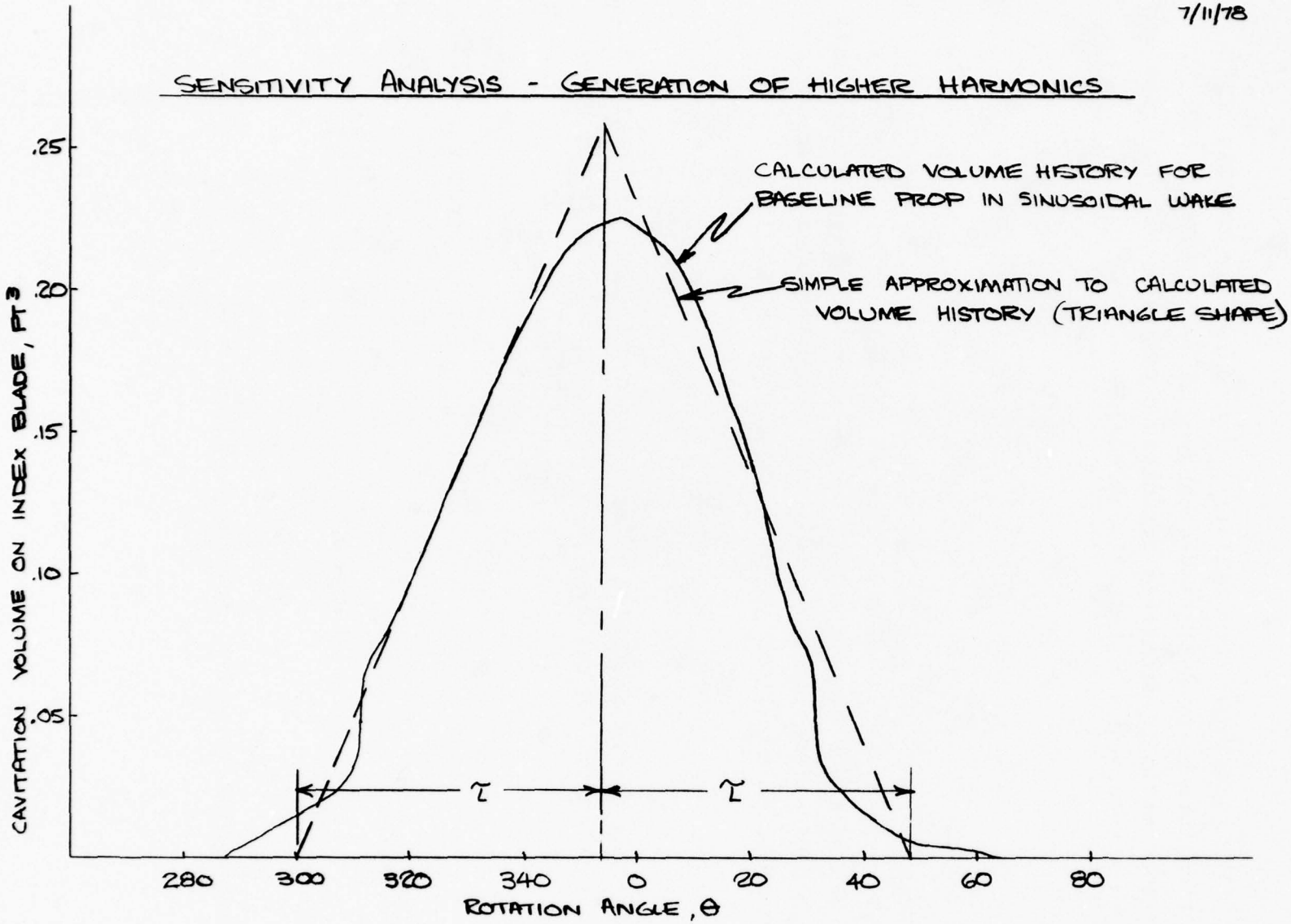

FIGURE 6.7

$$\langle p^2 \rangle \sim f_N^4 |A_N|^2$$

$$\sim \omega^4 F(\omega)^2$$

$$\sim \omega^4 \cdot \left(\frac{1}{\omega^2}\right)^2$$

$$\sim \text{Constant} \qquad (6.4)$$

So the upper *envelope* of the monopole source strengths at harmonics of blade rate will tend to be constant with frequency for the triangular volume history assumed. Since real volume histories will not have the sharp corners of this assumed triangular shape the higher harmonics will fall off eventually.

The above discussion and example demonstrate that the physical basis for the higher harmonics of blade rate is the nonlinear, threshold relationship between blade loading and cavity volume.

6.5 Ship Speed Reduction

The effect of ship speed reduction on the cavitation source strength is shown in Fig. 6.8 for the baseline propeller and wakefield. The effect is certainly substantial, amounting to a 30 dB reduction in source level for a 30% reduction in ship speed. This means that the speed at which ships are running (as a percentage of design speed) must be considered if ocean ambient noise from merchant shipping is to be properly estimated.

6.6 Blade Number

The effect of blade number on monopole source level is small for "equivalent" propellers, as shown by Fig. 6.9. For this sensitivity analysis "equivalent" propellers have been defined as having the same margin against back-bubble cavitation, a form of

SENSITIVITY ANALYSIS - EFFECT OF SHIP SPEED REDUCTION

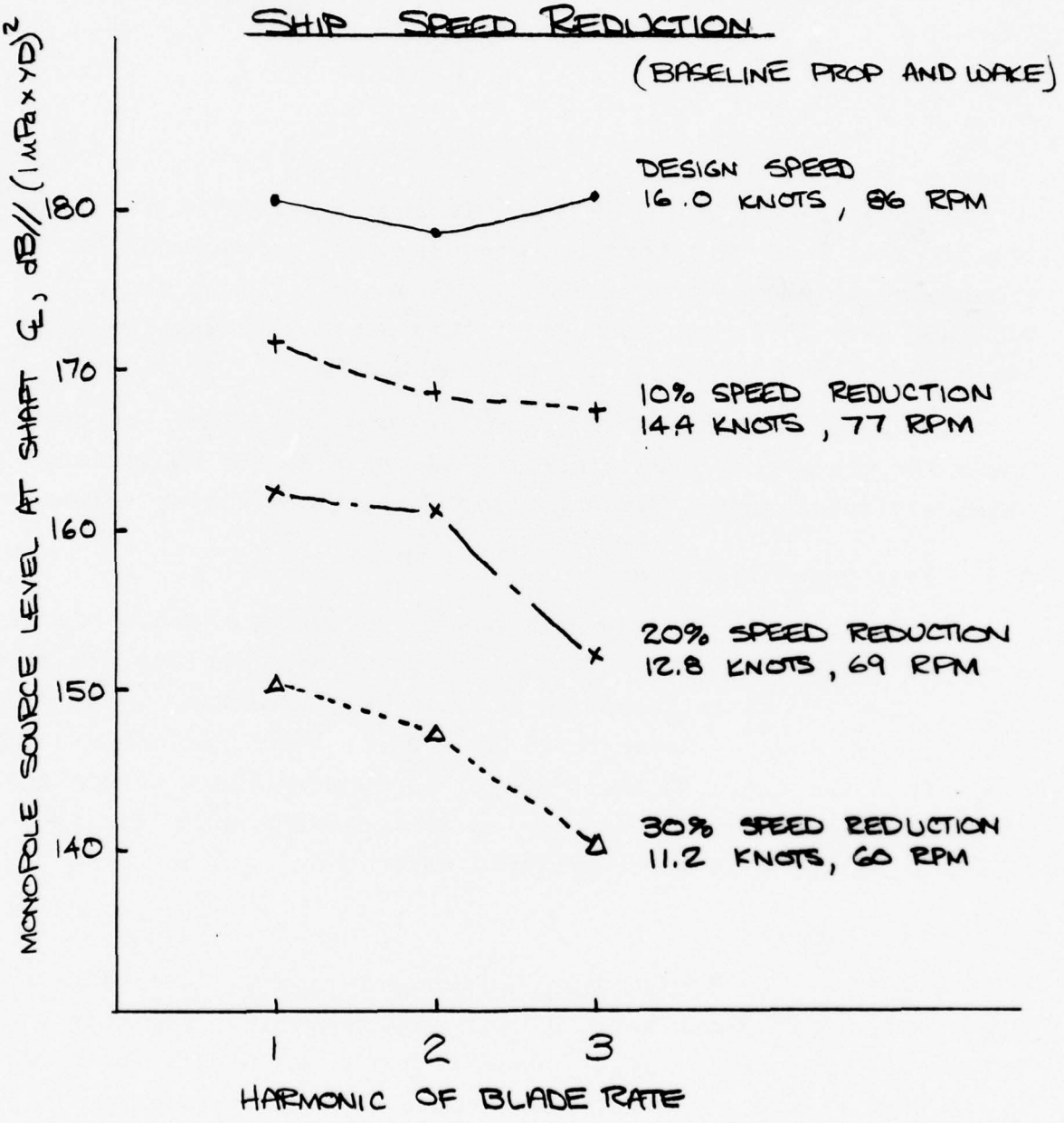

FIGURE 6.8

7/13/78
DSG

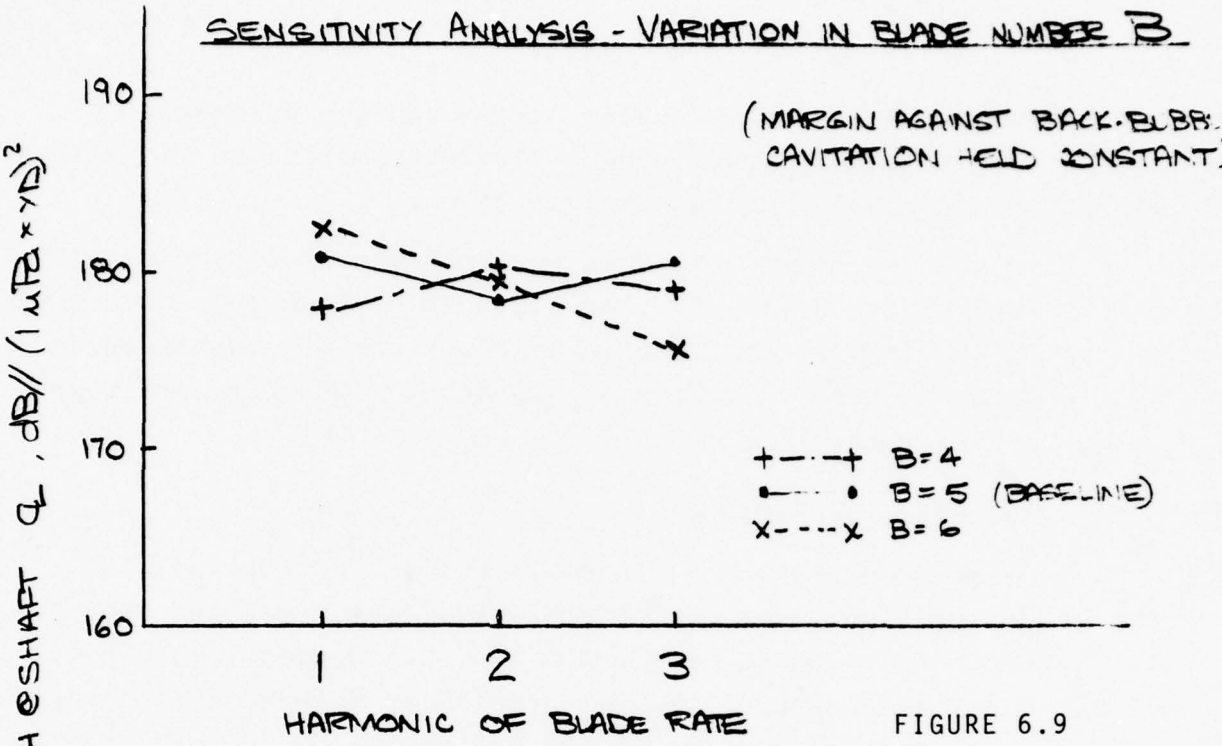

FIGURE 6.9

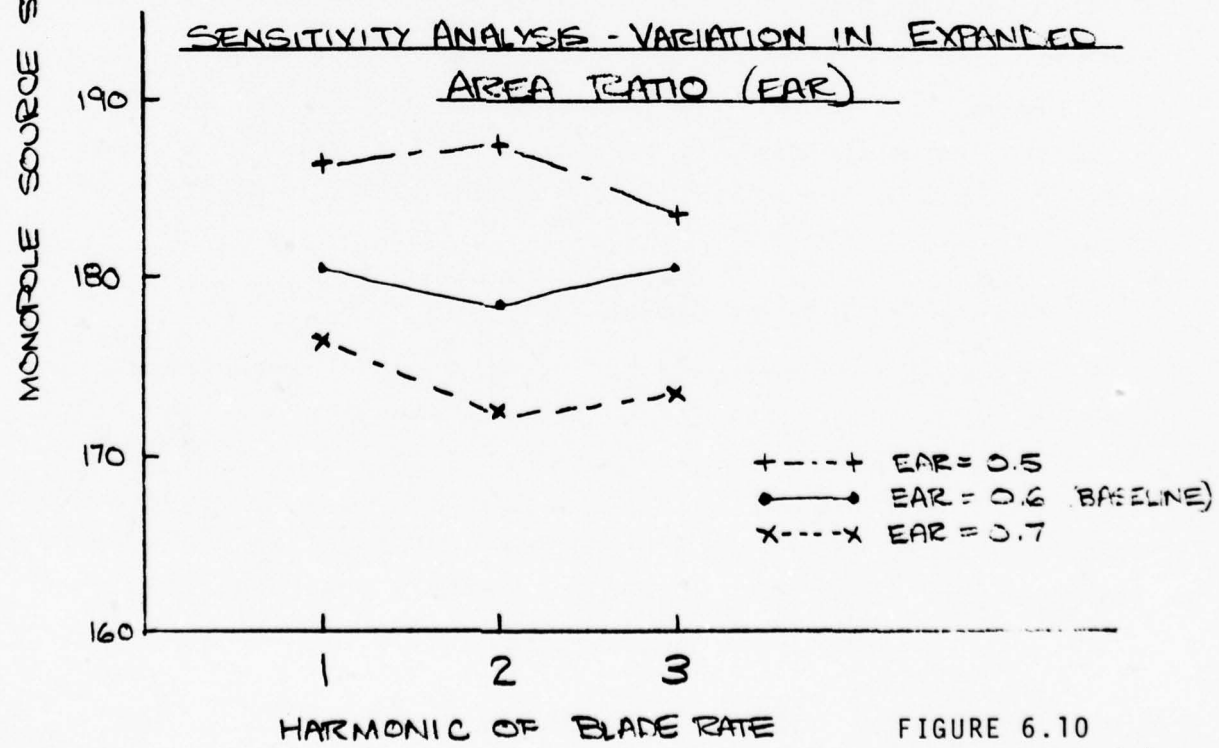

FIGURE 6.10

cavitation which generally causes severe erosion of propeller blades. This method of defining equivalent propellers is in line with standard naval architectural practice.

Although the monopole source strength does not vary significantly with blade number, the variation in blade number at constant propeller RPM implies a variation in blade rate frequency which will change the Lloyd mirror and consequently the pressure propagated to long ranges.

6.7 Expanded Area Ratio

The expanded area ratio (EAR) is defined as the ratio of the propeller blade area to the propeller disc area, and hence is just a non-dimensional measurement of blade area. The choice of EAR for a given propeller is a compromise between efficiency and cavitation considerations. The EAR should be as small as possible to minimize the viscous drag on the blades and hence maximize propeller efficiency. However, if the EAR is too small, cavitation will be excessive, leading to excessive noise and vibration and finally, thrust breakdown.

Figure 6.10 indeed shows that the effect of EAR on cavitation is quite large. Hence this variable must be properly modeled in order to predict the ocean ambient noise due to propeller cavitation.

6.8 Percentage Lift by Camber

A propeller is designed to suit the mean (circumferential average) wakefield. The design process consists of calculating the flow angle and lift coefficient at each radius so that the desired thrust or power absorption is obtained. The desired lift coefficient may be obtained by either cambering the blade or providing a flat blade with an angle of attack (see Fig. 2.3), or

SENSITIVITY ANALYSIS - VARIATION IN PERCENTAGE OF DESIGN LIFT BY CAMBER

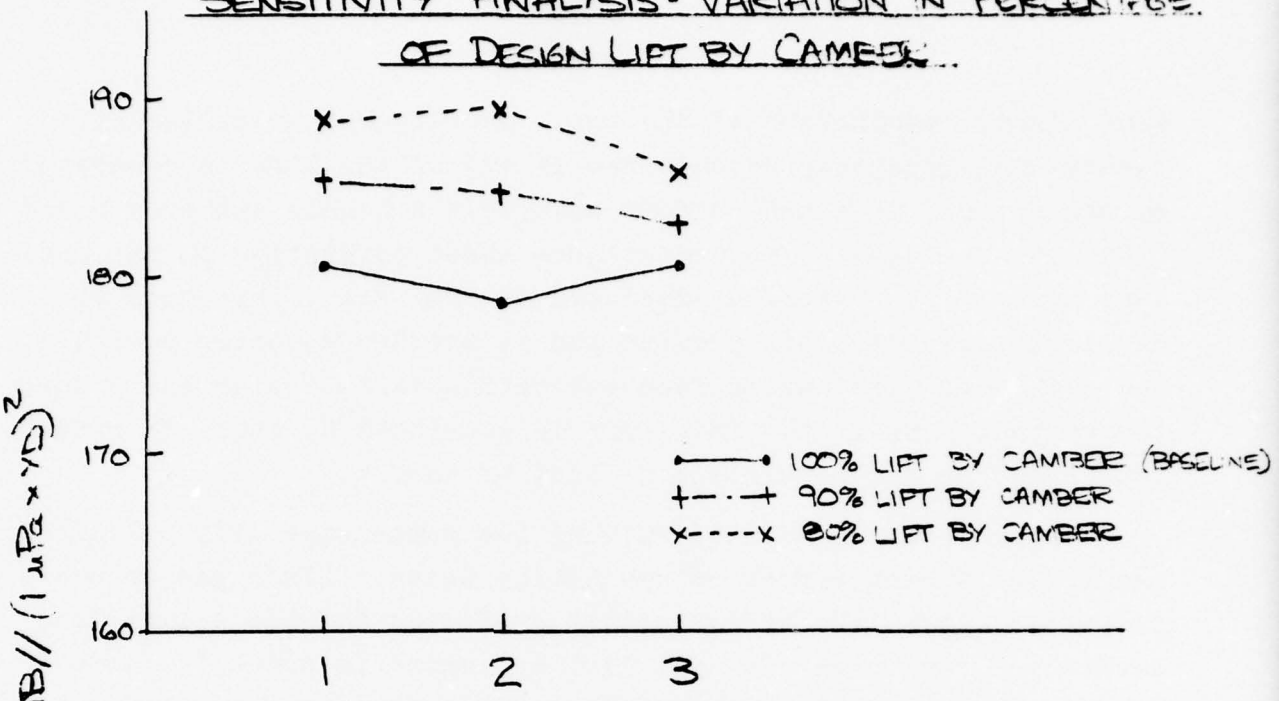

FIGURE 6.11

SENSITIVITY ANALYSIS - PITCH DISTRIBUTION

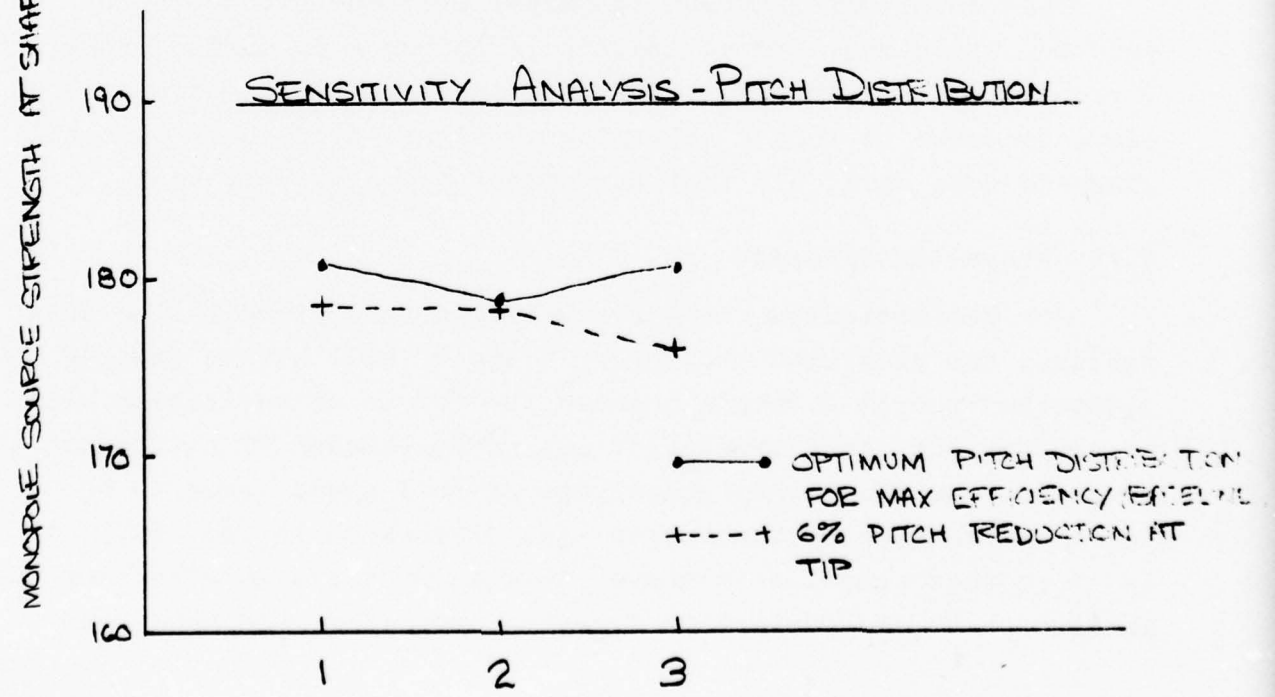

FIGURE 6.12

7/12/79
DSJ

some linear combination of the two. The highest propeller efficiency will generally be obtained if all of the lift is generated by camber, but in a non-uniform wakefield a highly cambered blade (100% lift by camber) may experience sheet cavitation on the pressure side of the blade, as depicted in Fig. 4.1. This form of cavitation causes blade erosion and is avoided whenever possible. One method of eliminating face cavitation is to design the propeller so that some of the mean lift is generated by angle of attack, thus reducing the percentage of lift by camber.

Figure 6.11 shows that varying the percentage lift by camber has a significant effect on cavitation noise. Since the baseline propeller (100% lift by camber) is predicted to have slight face cavitation, the prop with 90% lift by camber is probably closer to the propeller that would be found on a large tanker with a wakefield similar to the one used for the sensitivity analysis.

6.9 Pitch Distribution

The radial distribution of propeller blade pitch effects both the efficiency and cavitation performance of marine propellers. Current wisdom is to slightly reduce the pitch at the tip of the blade in order to reduce cavitation. Figure 6.12 shows that this approach does work, but that the effect is relatively small.

6.10 Propeller Diameter

For geometrically similar cavitation on different size propellers, the prop with the larger diameter will have a greater cavitation source strength because the volume of cavitation will be proportional to $(\text{diameter})^3$. Since the amount of cavitation present on merchant ship propellers at full speed *tends* to be constant fraction of blade area (see discussion in Sec. 6.7), it is clear that propeller diameter is a major variable affecting the cavitation volume present on a marine propeller, and hence the

acoustic source strength.

6.11 Design RPM

The effect of design RPM on "equivalent" propellers is fairly small, as shown by Fig. 6.14.

6.12 Design Shaft Horsepower (SHP)

Changing the design SHP while holding a constant margin against back bubble cavitation results in a comparatively small change in monopole source level. This is shown in Fig. 6.15.

6.13 Propeller Submergence

For a given propeller and wakefield, decreasing the depth of submergence will increase the amount of cavitation and thus the monopole source strength. For the example calculated for Fig. 6.16, decreasing the immersion to shaft centerline from 50 feet to 40 feet caused the blade rate source level to increase by 5 dB. Note, however, that this is for the same propeller and wakefield. If the prop were *designed* to operate at a shaft immersion of 40 feet then the expanded area ratio would have to be increased to keep the margin against back bubble cavitation the same, resulting in only a minor change in radiated noise. Hence the *design* submergence is not very important in determining cavitation noise (except for the change in Lloyd mirror), but the *operating* submergence of a given propeller can be important. This depends on whether a ship is operating in the loaded condition or in the ballast condition.

6.14 Wakefields

The baseline propeller was analyzed in several different wakefields, each of which has the same circumferential average velocities, so that the mean propeller loading remains constant.

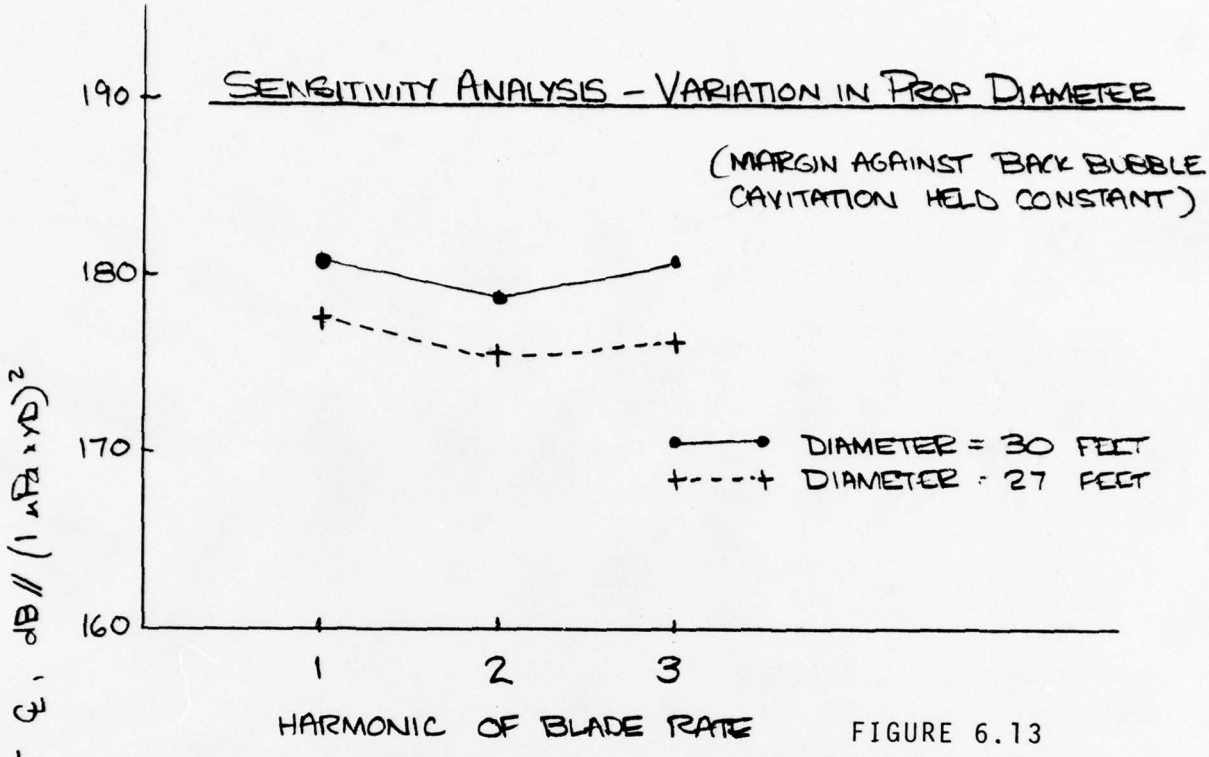

FIGURE 6.13

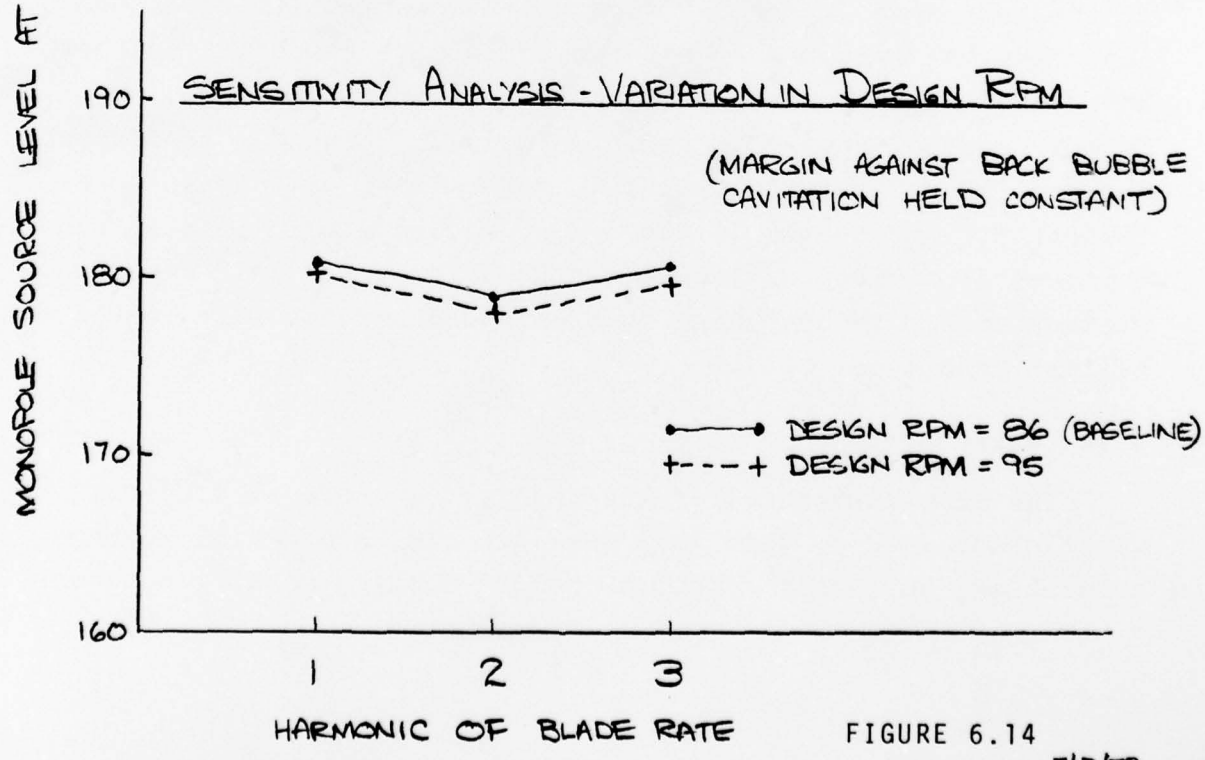

FIGURE 6.14

7/13/78
DSG

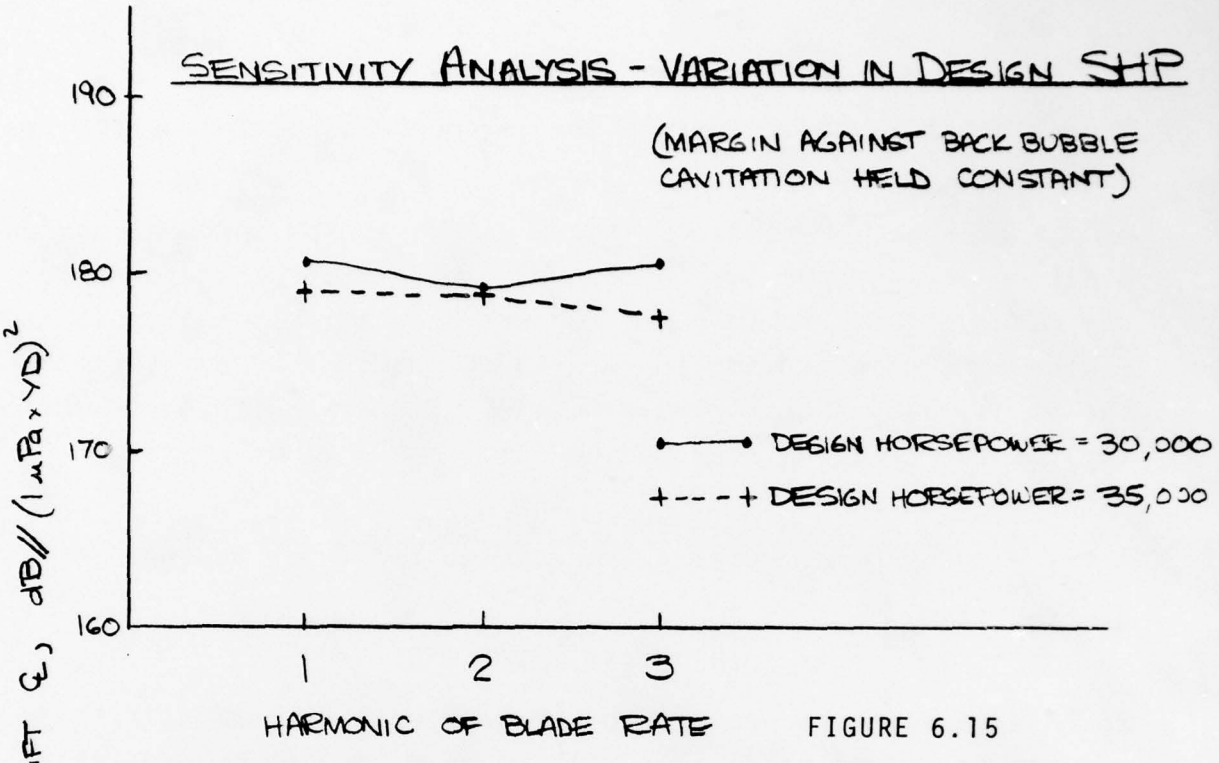

FIGURE 6.15

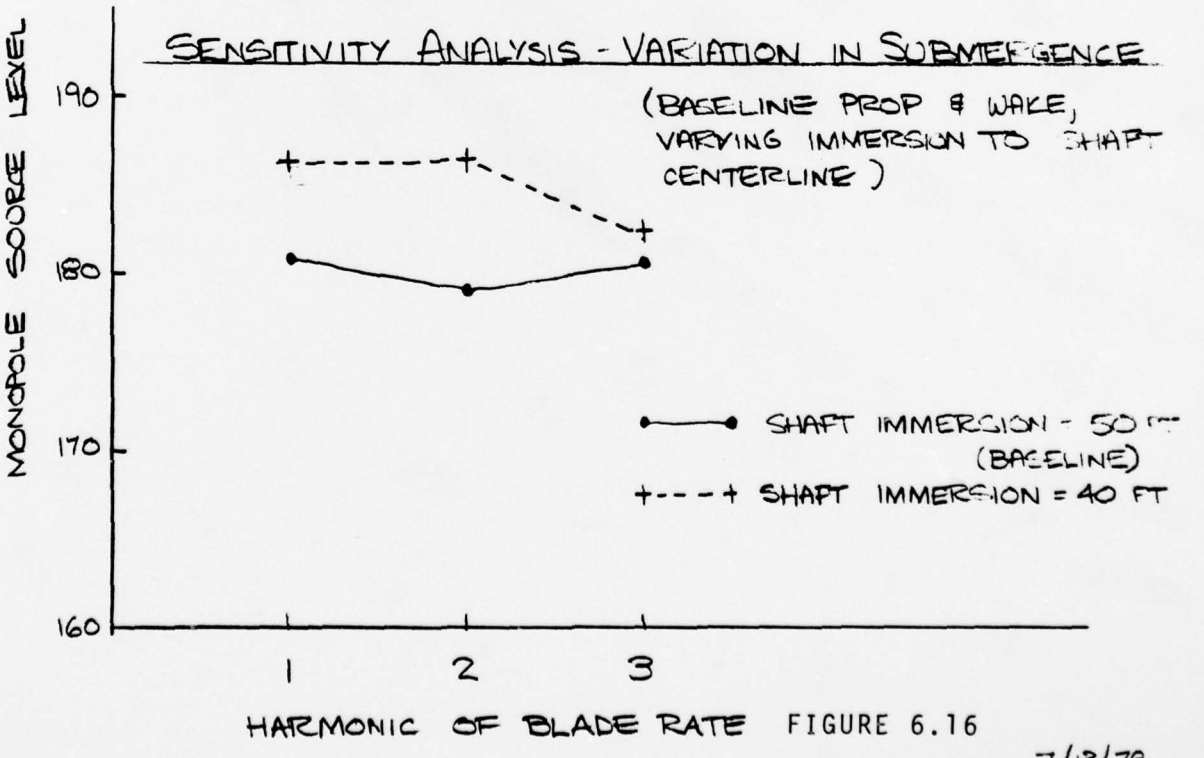

FIGURE 6.16

7/13/78
DSG

The wakefields vary only in their degree of circumferential non-uniformity.

The propeller blade cavitates mainly in the vertical upright position because the low inflow velocities present there cause the blade loading to increase. Hence the inflow velocity in this region is a major factor influencing the amount of cavitation on the blade, and an appropirate measure of the wakefield non-uniformity (as it influences cavitation) is

$$\frac{\text{Minimum Velocity at 0.9 Radius (At } \theta=0^{\circ})}{\text{Circumferential Average Velocity At 0.9 Radius}} ,$$

denoted

$$(V_{MIN}/V_{AVG}).9R .$$

If this quantity is unity then the wake will be perfectly uniform and the transient cavitation will go away completely. As this quantity becomes smaller, the intermittent blade loading will increase, which will cause the volume of unsteady cavitation to increase.

Figure 6.17 shows the estimated cavitation source levels for the baseline propeller running in different wakefields. The correlation between $(V_{MIN}/V_{AVG}).9R$ and source level is clear. This confirms our previous conclusion that wakefield non-uniformities play a primary role in determining the cavitation source strength of merchant ship propellers.

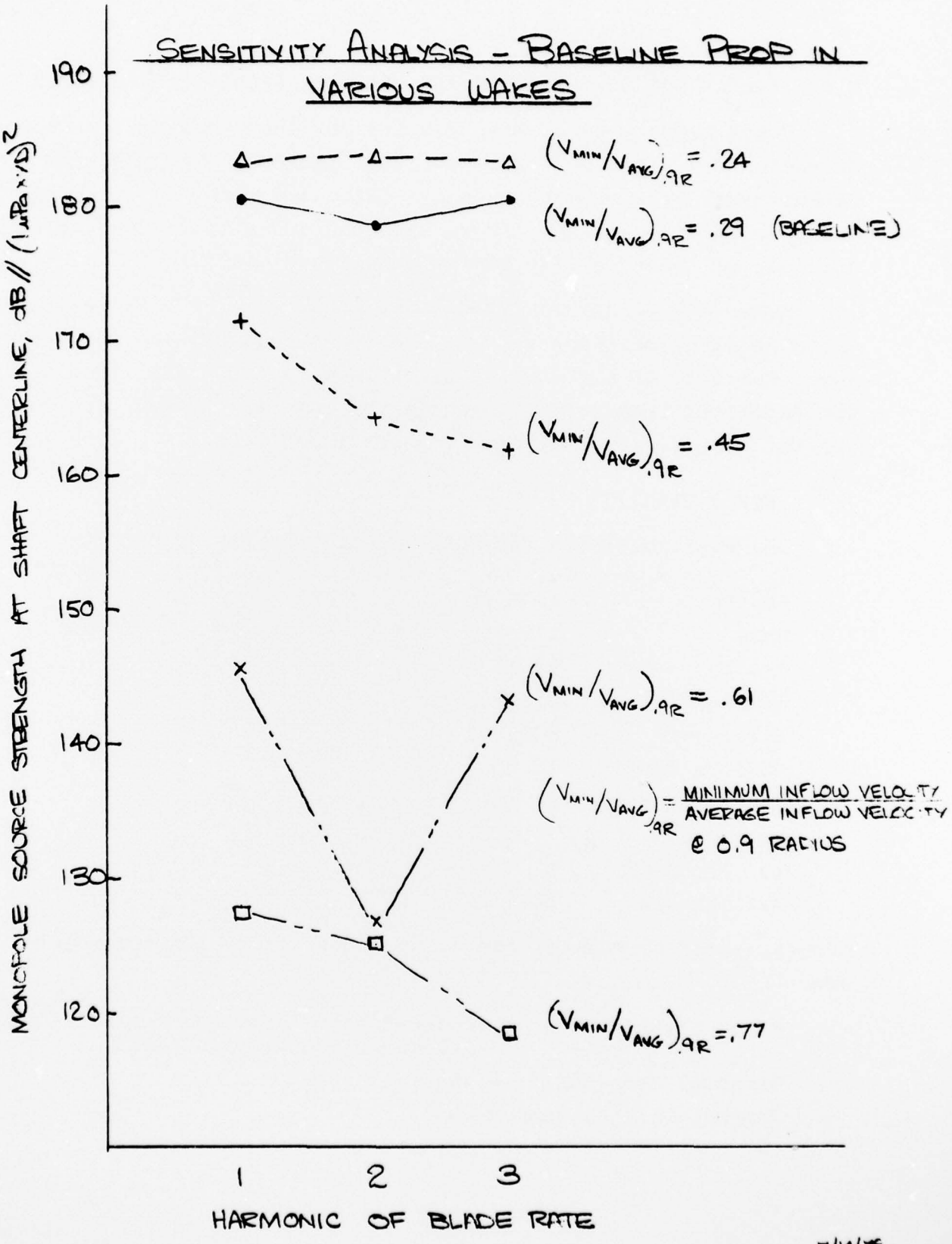
SENSITIVITY ANALYSIS - BASELINE PROP IN VARIOUS WAKES
MONOPOLE SOURCE STRENGTH AT SHAFT CENTERLINE, dB // (1 μPa x 1 ft)²
190
180
170
160
150
140
130
120
1
2
3
HARMONIC OF BLADE RATE
(VMIN/VAVG).9R = .24
(VMIN/VAVG).9R = .29 (BASELINE)
(VMIN/VAVG).9R = .45
(VMIN/VAVG).9R = .61
(VMIN/VAVG).9R = .77
(VMIN/VAVG).9R = MINIMUM INFLOW VELOCITY / AVERAGE INFLOW VELOCITY @ 0.9 RADIUS
7/14/78
DSG

FIGURE 6.17

7.0 COMPARISON OF PREDICTED AND MEASURED ACOUSTIC SIGNATURES

Comparisons between measured and predicted cavitation source strengths are given here for two large tankers. The acoustic measurements were made by Cybulski (Ref. 18). The data for these ships is rather sketchy, and we have had to estimate the wakefield and some of the propeller design specifications.

Since the WORLD DIGNITY and the LAGENA are both approximately the same size and shape we have assumed the wakefields to be the same, for lack of any more detailed information. The wakefield was estimated from Ref. 17, and is the same as the wakefield used for the sensitivity analysis (Figs. 6.1 and 6.2).

7.1 WORLD DIGNITY

The available data for WORLD DIGNITY is listed below.

Length	1100 ft
Beam	175 ft
Draft	68 ft
Tonnage	271,000 tons deadweight
Horsepower	~30,000
Maximum Speed	16.0 knots
Prop Diameter	30 ft
Prop Depth to ℄	~50 ft
No. of Blades	5
Maximum RPM	86

Our estimates of some of the other propeller design parameters are

Pitch Distribution - reduced pitch at blade tip relative to optimum pitch distribution

Expanded Area Ratio - .60

Percent Lift by Camber - 95%

The predicted source level for the first three harmonics of blade rate are shown in Fig. 7.1, along with the source levels as inferred from acoustic measurements (Ref. 18). We have not shown predicted levels at the higher harmonics because the influence of bubble dynamics and the tip vortex cavity volume on the higher harmonics have not yet been investigated. We feel that a comparison between predicted and measured levels at these higher harmonics would be premature at the present time.

It is seen that the predicted blade rate level is 12 dB below the measured level, while the second and third harmonics are in fairly good agreement (1-2 dB too high). The discrepancy at blade rate may be due to hull vibration augmenting the radiation, as discussed in Section 7.3.

7.2 LAGENA

The major characteristics of the tanker LAGENA are very similar to those of the WORLD DIGNITY, and hence will not be repeated here. The major difference is that the LAGNEA has a 4-bladed prop, while the WORLD DIGNITY has a 5-bladed propeller. This will affect the blade rate frequency.

The comparison between predicted and measured source levels for the LAGENA is shown in Figure 7.2. Again the discrepancy is largest at blade rate (17 dB) and decreases with increasing harmonic number.

7.3 Influence of Hull Vibration

There are several factors which suggest that hull vibration of very large ships is augmenting the radiation from the cavity volume fluctuations at low frequencies (blade rate and twice blade rate):

7/18/78
DSG

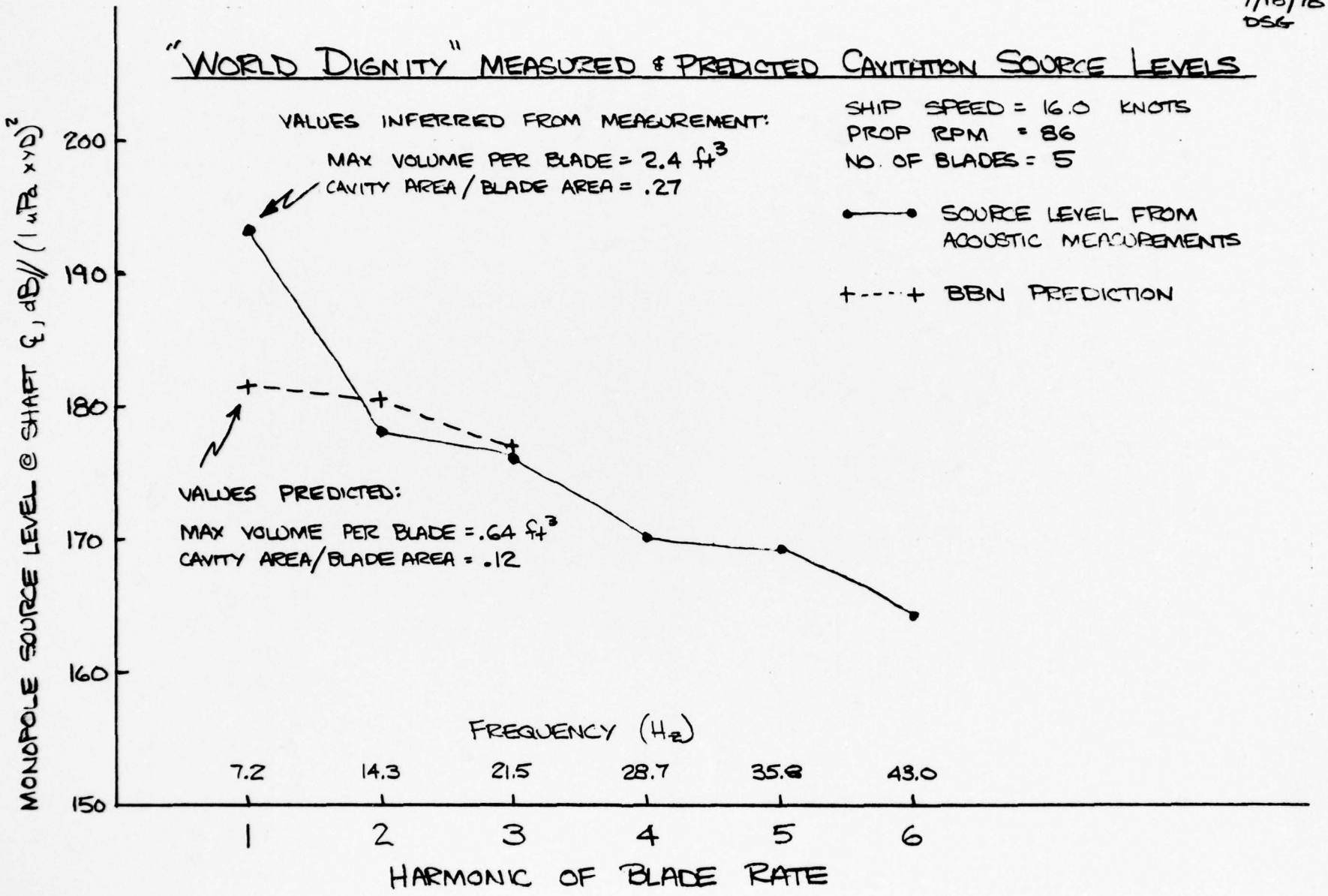

FIGURE 7.1

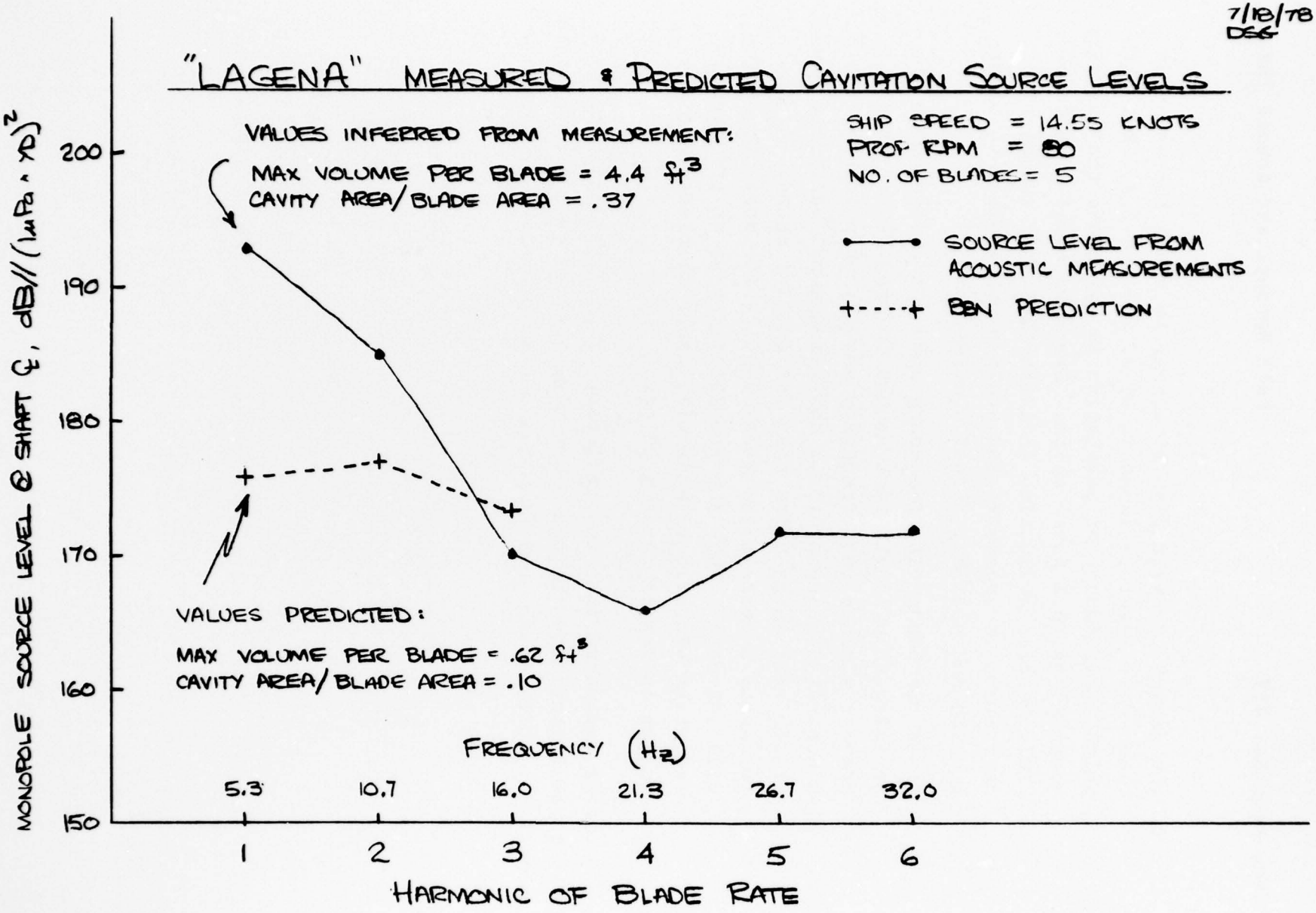
7/18/78
DSG
"LAGENA" MEASURED & PREDICTED CAVITATION SOURCE LEVELS
VALUES INFERRED FROM MEASUREMENT:
MAX VOLUME PER BLADE = 4.4 ft³
CAVITY AREA/BLADE AREA = .37
SHIP SPEED = 14.55 KNOTS
PROP RPM = 80
NO. OF BLADES = 5
SOURCE LEVEL FROM ACOUSTIC MEASUREMENTS
BBN PREDICTION
VALUES PREDICTED:
MAX VOLUME PER BLADE = .62 ft³
CAVITY AREA/BLADE AREA = .10
MONOPOLE SOURCE LEVEL @ SHAFT ℄, dB// (1μPa · yd)²
200
190
180
170
160
150
FREQUENCY (Hz)
5.3
10.7
16.0
21.3
26.7
32.0
1
2
3
4
5
6
HARMONIC OF BLADE RATE

FIGURE 7.2

- The amount of cavitation necessary to cause the measured blade rate level is shown in Figs. 7.1 and 7.2. For both ships, this amount of cavitation is far above that usually observed on full scale ships. Standard naval architectural practice would also indicate that this amount of cavitation is excessive and would probably lead to blade erosion and possibly thrust breakdown.
- Since the blade rate frequency does not go down with increasing ship length fast enough to keep fL = constant, where f = blade rate frequency and L = ship length, the blade rate frequency (on a non-dimensional basis) is higher for very large ships than for smaller ships. As the frequency increases the modal density for most structures will increase. Thus the probability that an efficiently radiating vibrational mode will occur at blade rate frequency is larger for big ships.

It is suggested that the influence of hull vibration on radiation be investigated before exercising the cavitation prediction model to predict ocean ambient noise due to propeller cavitation.

8.0 CONCLUSIONS

a) The present method of calculating sheet cavitation volume-time histories appears to be adequate for determining the cavitation source level at the first few harmonics of blade rate.

b) The major cause of cavitation noise at the higher harmonics of blade rate is the highly non-linear relationship between blade loading and cavitation volume.

c) The details of the volume history will affect the generation of noise at the higher harmonics of blade rate. The influence of bubble dynamics and the volume associated with a cavitated tip vortex will have to be investigated before we can confidently predict the source level at higher harmonics of blade rate.

d) The major *design* variables which influence the cavitation source level are:

- o diameter
- o expanded area ratio (EAR)
- o percentage lift by camber

The major operational variables which influence cavitation source level are:

- o wakefield non-uniformities
- o ship speed (as a percentage of design speed)
- o shaft immersion

e) The estimation of the wake non-uniformities which the full-scale propeller experiences is extremely difficult. Although wake surveys are commonly made on ship models, the full scale effective wakefield may be quite different from that measured during a model wake survey for two reasons:

- The large Reynolds number difference between model and full scale
- The pressure field associated with a working propeller substantially alters the flow over the stern of the ship, and hence the non-uniformities of the wakefield.

f) The presence of the hull may affect the radiation from the cavitation volume fluctuations. The effect may be either to augment or decrease the radiation, depending on the frequency and the construction of the ship. This may explain the extremely high blade rate source levels observed on large tankers.

g) All of the propellers investigated in the present work showed significant cavitation only when the blade was near the vertical upright ($\theta=0^{\circ}$) position. This implies that the proper source depth for cavitation volume fluctuations is near thetip of the blade in the upright position, rather than at the shaft centerline.

9.0 RECOMMENDATIONS

a) The influence of bubble dynamics and tip vortex cavitation on the cavitation noise at higher harmonics of blade rate should be investigated.

b) The effect of hull vibration on the radiation from a cavitation volume source must be determined, either analytically or experimentally.

c) The numerical discretization errors in the present computer program which tend to generate high harmonics need to be remedied.

d) Any improvements to the computer program which will reduce the cost of using it should be incorporated before exercising the program to predict the ensemble characteristics of the ocean ambient noise due to propeller cavitation.

REFERENCES

1) Gray, L.M., Greeley, D.S., "Estimation of Propeller Cavitation Volume Velocity for Merchant Vessels", BBN Tech Memo No. 319, February 1977.

2) BBN Presentation to NRL (B. Adams and O. Diachok), December 1977.

3) Brown, N.A., "Periodic Propeller Forces in Non-Uniform Flow", MIT Report 64-7, June 1964.

4) Sasajima, T., "Usefulness of Quasi-Steady Approach for Estimation of Propeller Bearing Forces", Paper presented at Propellers '78 Symposium, SNAME, 1978.

5) Tsakonas, S. *et al*, "Propeller Blade Pressure Distribution Due to Loading and Thickness Effects", Davidson Laboratory Report 1869, April, 1976.

6) Abbot, I.H., von Doenhoff, A.E., "Theory of Wing Sections", Dover Publications, 1959.

7) Brockett, T., "Minimum Pressure Envelopes for Modified NACA-66 Sections with NACA a=0.8 Camber and BUSHIPS Type I and Type II Sections", DTMB Report 1780, February 1966.

8) Greeley, D.S., "Propeller Optimization in Inclined Flow", B.S. Thesis, Webb Institute of Naval Architecture, 1976.

9) Geurst, J.A., "Linearized Theory of Partially Cavitated Hydrofoils", Intern. Ships. Progr. 6, No. 60, pp. 369-384.

10) Geurst, J.A., "Linearized Theory for Fully Cavitated Hydrofoils", Intern. Shipb. Progr. 7, No. 65, pp. 17-27.

11) Geurst, J.A. and Verbrugh, P.J., "A Note on the Camber Effects of a Partially Cavitated Hydrofoil", Intern. Shipb. Progr. 6, No. 61, pp. 409-414.

12) Noordzij, L., "Pressure Field Induced by a Cavitating Propeller", Intern. Shipb. Progr. 23, No. 260, pp. 93-105.

13) Noordzij, L. and Officier, M.J., "The Effect of Camber on the Pressure Field of a Super Cavitating Propeller", Intern. Shipb. Progr. 24, No. 273, pp. 115-121.

14) Oossanen, P. van, "Calculation of Performance and Cavitation Characteristics of Propellers Including Effects of Non-Uniform Flow and Viscosity", NSMB Publication 457, 1974.

15) Oossanen, P. van, "Theoretical Prediction of Cavitation on Propellers", Marine Technology Vol. 14, No. 4, Oct. 1977.

16) Ross, D., "Mechanics of Underwater Noise", Pergamon Press, 1976.

17) Gray, L.M. and Greeley, D.S., "A Generalized Model for Predicting the Wake Field of Merchant Vessels", BBN Tech Memo No. 279, February 1977.

18) Cybulski, J., "Probable Origins of Measured Supertanker Radiated Noise Spectra", Oceans '77 Conference Record, Vol. 1, October 1977.